

# Strontium Isotopic Stratigraphy of the Miocene Adana Basin (S. Anatolia) and its Geological Implications

Ahmet Can Akinci<sup>1,\*</sup>

<sup>1</sup> Çukurova University, Faculty of Engineering, Department of Geological Engineering, Adana, Turkey; (\*corresponding author: acakinci@cu.edu.tr)

doi: 10.4154/gc.2025.05



## Article history:

Manuscript received: April 25, 2024

Revised manuscript accepted: December 05, 2024

Available online: February 27, 2025

## Abstract

This paper presents the first  $^{87}\text{Sr}/^{86}\text{Sr}$  data and its geological implications for the entire stratigraphic sequence of the Neogene Adana Basin, one of the largest basins in southern Turkey (eastern Mediterranean). The Adana Basin is strategically located near the convergence point of the African, Arabian, and Anatolian plates, making it vital for understanding the regional geological history. In this study, 15 systematically collected samples from six different formations within the Adana Basin were subjected to strontium isotope analysis ( $^{87}\text{Sr}/^{86}\text{Sr}$ ). The results were presented and interpreted for all units except the Handere Formation (Messinian fluvial, shallow marine-lagoon deposits). Notably, some of the corresponding ages of the recorded  $^{87}\text{Sr}/^{86}\text{Sr}$  results have contradicted the published biostratigraphic ages from the literature. To explain the observed deviations in the Güvenç and Kuzgun formations, geochemical, petrographic, and SEM analyses were conducted, revealing that these deviations are generally related to diagenetic alteration and the high detrital content of the units. Additionally, fundamental palaeontological studies were carried out to provide supporting information. The  $^{87}\text{Sr}/^{86}\text{Sr}$  deviations observed in the shallow marine units can be attributed to multiple factors, including short-term sea-level fluctuations, continental run-off, terrestrial feeding/riverine input, and volcanic activity during the late Tortonian–Messinian period. New field observations combined with  $^{87}\text{Sr}/^{86}\text{Sr}$  data enabled the differentiation of distinct reef carbonates with similar lithologies. These findings demonstrate the formation of various reef levels through multiple short-term phases alongside a gradual regression of sea level in the basin during the late Miocene period.

**Keywords:** Adana Basin,  $^{87}\text{Sr}/^{86}\text{Sr}$ , stratigraphy, Neogene

## 1. INTRODUCTION

The Neogene Adana Basin, located in southern Turkey, holds significant geological importance due to its proximity to the triple junction of the Arabian, African, and Anatolian plates. It is believed that the basin developed as a result of extensional tectonics caused by the southward rollback of the African plate, as proposed by ROBERTSON (1998). Over the years, numerous general geological-stratigraphic studies have been conducted in the region by researchers such as SCHMIDT (1961), YETİŞ & DEMİRKOL (1986), YETİŞ et al. (1986), ÜNLÜGENÇ & DEMİRKOL (1988) and ÜNLÜGENÇ (1986, 1993). Detailed discussions on the general stratigraphy and geology of the Adana Basin were presented by YETİŞ (1988) and ÜNLÜGENÇ (1993), revealing its main sedimentary and tectonic characteristics. More recently, NURLU et al. (2021) reported  $^{87}\text{Sr}/^{86}\text{Sr}$  analysis for carbonatic tuffites in the Kuzgun Formation, providing ages between 20 and 27 Ma, corresponding to the Burdigalian–Chattian period. They suggested that these tuffites were originally deposited during the Middle–Upper Miocene and were later transported from a northerly source area.

The basis of Sr isotope stratigraphy lies in the assumption that the  $^{87}\text{Sr}/^{86}\text{Sr}$  of seawater is relatively constant throughout the earth's oceans, with residence times of Sr in seawater ranging from approximately 2.5 to 5 million years (BROEKER & PENG, 1982; MCARTHUR, 1994) or even less (KUZNETSOV

et al., 2012), which is significantly greater than the mixing time of the ocean (approximately  $10^3$  years). The study of Sr-isotope ( $^{87}\text{Sr}/^{86}\text{Sr}$ ) variations in Cenozoic seawater was first described by BURKE et al. (1982) and further improved by KOEPNICK et al. (1985, 1988) and ELDERFIELD (1986). Since then, the Neogene Sr-isotope seawater curve has received considerable attention and has been investigated by various researchers (HODELL & WOODRUFF, 1994; OSLICK et al., 1994). These advancements have led to the establishment of a detailed marine Sr-isotope chronology for Neogene basins, based on high precision measurements. Consequently, stratigraphic studies, primarily reliant on palaeontology and relative dating, can now be supported by a chemical quantitative method based on the Sr isotope composition of sediments. This chemical approach has opened new avenues for understanding the geochronological development of basins. However, it is important to consider factors such as chemical weathering, soil formation, and seasonal alterations that can affect the Sr isotopic composition in deposits (CAI et al., 2020). The dissolution of minerals including biotite, feldspar, and plagioclase under different intensities of chemical weathering can lead to variable  $^{87}\text{Sr}/^{86}\text{Sr}$  contents in water and sediment (YANG et al., 2007). Despite these challenges, unexpected deviations in  $^{87}\text{Sr}/^{86}\text{Sr}$  ratios remain crucial indicators for assessing diagenetic processes in rock units, salinity reconstructions, sediment sources, and palaeo-environmental evaluations (VEIZER, 1983; MCARTHUR et

al., 2001; YANG et al., 2007; WIERZBOWSKI, 2013; SCHILDGEN et al., 2014).

This paper aims to present the first strontium isotopic composition ( $^{87}\text{Sr}/^{86}\text{Sr}$ ) and its geological implications for the deposits from the Adana Basin. The available age determinations were primarily based on micro-palaeontological studies with limited single-unit (even member) isotopic determinations. Strontium isotope stratigraphy of basin sediments, besides determining the age of the sample in question, allows facies correlations and provides more detailed data about the basin's evolution. In this study, the obtained  $^{87}\text{Sr}/^{86}\text{Sr}$  compositions of the units outcropping in the Adana Basin are compared with the literature and are interpreted to provide a foundation for further research. In addition, data pertaining to late Miocene reefal sedimentation in the basin and probable episodic relative sea-level changes during the Tortonian–Messinian period (ILGAR et al., 2013), resulting in transgressive sedimentation, are discussed.

## 2. Geological Setting and Stratigraphy

The Adana Basin was developed on the Palaeozoic and Mesozoic basement units that form a south-verging imbricate thrust stack in the south of the Taurus Mountain Belt in southern Anatolia (BURTON-FERGUSON et al., 2005). The Adana Basin is separated from the İskenderun Basin by the NE-SW trending Misis Mountain Range in the south. The basin hosts a nearly 6000 m thick sedimentary succession, spanning rock units from the Miocene to the recent (BURTON-FERGUSON et al., 2005). According to the latest geodynamic models, the Adana Basin lies above the zone of Cenozoic suturing between the Afro-Arabian and Eurasian plates (DEWEY & ŞENGÖR, 1979; ŞENGÖR & YILMAZ, 1981; ROBERTSON & DIXON, 1984; GEALEY, 1988; KAHLE et al., 2000; REILINGER et al., 2010; MAHMOUD et al., 2013).

The timing of the collision between the Arabian and Anatolian plates has been debated. Some suggest it occurred during the late Cenozoic (KELLING et al., 1987) or middle Miocene (ŞENGÖR, 1979; ŞENGÖR & YILMAZ, 1981; DEWEY et al., 1986). More recent studies propose an Eocene–Miocene age (HEMPTON, 1985; YILMAZ, 1993). This extension stretches from the Mediterranean Sea to Kyrenia. Following the continental collision, the continued northward movement of the Arabian Plate along the Southeastern Anatolian Orogenic Belt resulted in intense compressional deformation, thickening the eastern Anatolian crust. Further shortening in the region led to the formation of two major fault zones namely the North Anatolian Fault Zone (NAFZ) and the East Anatolian Fault Zone (EAFZ) (ALBORA et al., 2006; BARKA & KADINSKY-CADE, 1988; PERİNÇEK & ÇEMEN, 1990).

Within this tectonic framework, the Neogene sequence of the Adana Basin fill is represented by seven formations (Figs. 1, 2) representing different facies characteristics, and developed just south of the eastern Taurus Mountain range. It has been reported that these formations were deposited due to extensive subsidence in the basin during the early and middle Miocene (ÜNLÜGENÇ & AKINCI, 2020). This thick sedimentary sequence can be divided into pre-transgressive, transgressive,

and regressive sequences. The pre-transgressive Gildirli Formation was deposited during the late Oligocene–early Miocene and is exposed on the northern flank of the basin (ÜNLÜGENÇ, 1993; ÜNLÜGENÇ & AKINCI, 2020). During the early Miocene, the Adana Basin experienced rapid subsidence driven by extensional tectonics, leading to marine incursions and gradual sedimentary infilling. This was followed by a significant northward marine transgression during the Langhian–Serravallian, resulting in a thick sedimentary accumulation. By the Tortonian–Messinian, subsidence decreased, indicating a shift in sediment transport regimes due to tectonic uplift and sea-level changes. Late Miocene to Pliocene compressional events further reshaped the basin, influenced by sinistral fault movements that defined its current structure (ÜNLÜGENÇ, 1986, 1993; ÜNLÜGENÇ & DEMİRKOL, 1988; ÜNLÜGENÇ & AKINCI, 2020; AKINCI & ÜNLÜGENÇ, 2021; AKINCI et al., 2023).

A possible marine inundation from the south during the early Miocene led to the deposition of a transgressive sequence, including the Kaplankaya, Karaisalı, Cingöz, and Güvenç Formations which make up most of the Adana Basin fill (ÜNLÜGENÇ, 1993; ÜNLÜGENÇ & AKINCI, 2020). While the Kaplankaya and Karaisalı Formations characterise the main Miocene shallow-marine/platform deposits in the Adana Basin, the turbiditic Cingöz Formation represents sedimentation in the deeper parts of the basin (ÖZÇELİK & YETİŞ, 1994). The Kaplankaya Formation includes a wide range of facies deposited in the shallow parts of the basin along with the reefal Karaisalı Formation. The Güvenç Formation, which is generally dominated by lithologies including shale and mudstone, covers the fore reef, deep sea, and shallow sea facies stratigraphically from bottom to top (ÖZÇELİK & YETİŞ, 1994). The Kuzgun Formation, which overlies the Güvenç Formation with a low-angle unconformity, began with levels consisting of coastal, beach, and meandering river sediments, indicating the early stages of the regressive period in the basin (ÜNLÜGENÇ et al., 2019). ILGAR et al. (2013), suggesting that a short-lived relative sea level rise that led the shallow-marine sedimentation in the early Tortonian was accompanied by a second generation of reefal limestones along the basin margin (Fig. 2). The Messinian–Pliocene Handere Formation consists of sandstone, siltstone, and terrestrial sediments including marl and gypsum. It overlies the Kuzgun Formation with a low-angle unconformity and is, in turn, unconformably overlain by Quaternary Terrace–Caliche and Alluvium deposits (ÜNLÜGENÇ, 1993; SINACI, 2010; ŞAFAK et al., 2021).

### 2.1. The Gildirli Formation

The Gildirli Formation is a pre-transgressive continental conglomeratic unit, underlying the Miocene sediments of the Adana Basin (ÜNLÜGENÇ, 1993; DERMAN & GÜRBÜZ, 2007). This formation crops out around the Akdam, Gildirli, and Karakılıç villages and is dominated by alternations of conglomerate, sandstone, shale, and mudstone. The unit is observed to fill the irregular pre-Miocene topography formed by Mesozoic and Palaeozoic rock units. Conglomerates and other clastic sediments within the unit are generally alluvial in character and present a distinct reddish colour. The reddish-brown, thick to very thick-bedded conglomerates display

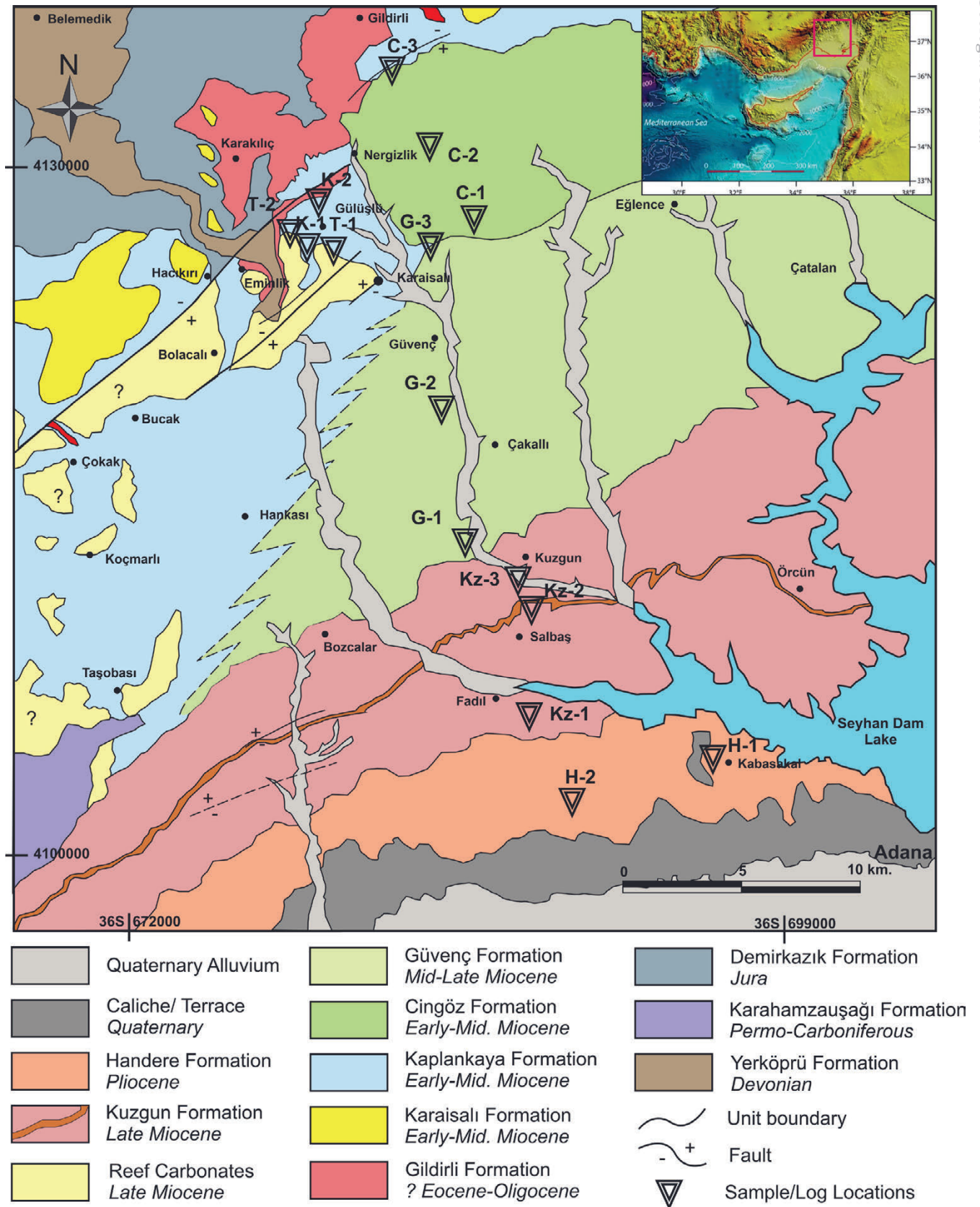


Figure 1. Geological map of the study area (modified after ÜNLÜGEnÇ, 1993). Sampling/sedimentary log locations for strontium analyses are indicated on the map.

cross-bedding and include well rounded, poorly sorted pebbles which are derived from Palaeozoic–Mesozoic carbonates and ophiolites. The Gildirli Formation unconformably overlies the

Oligocene lacustrine deposits of the Karsanti Formation in the Çökak area and is transitionally overlain by the Kaplankaya and Karaisalı Formations.

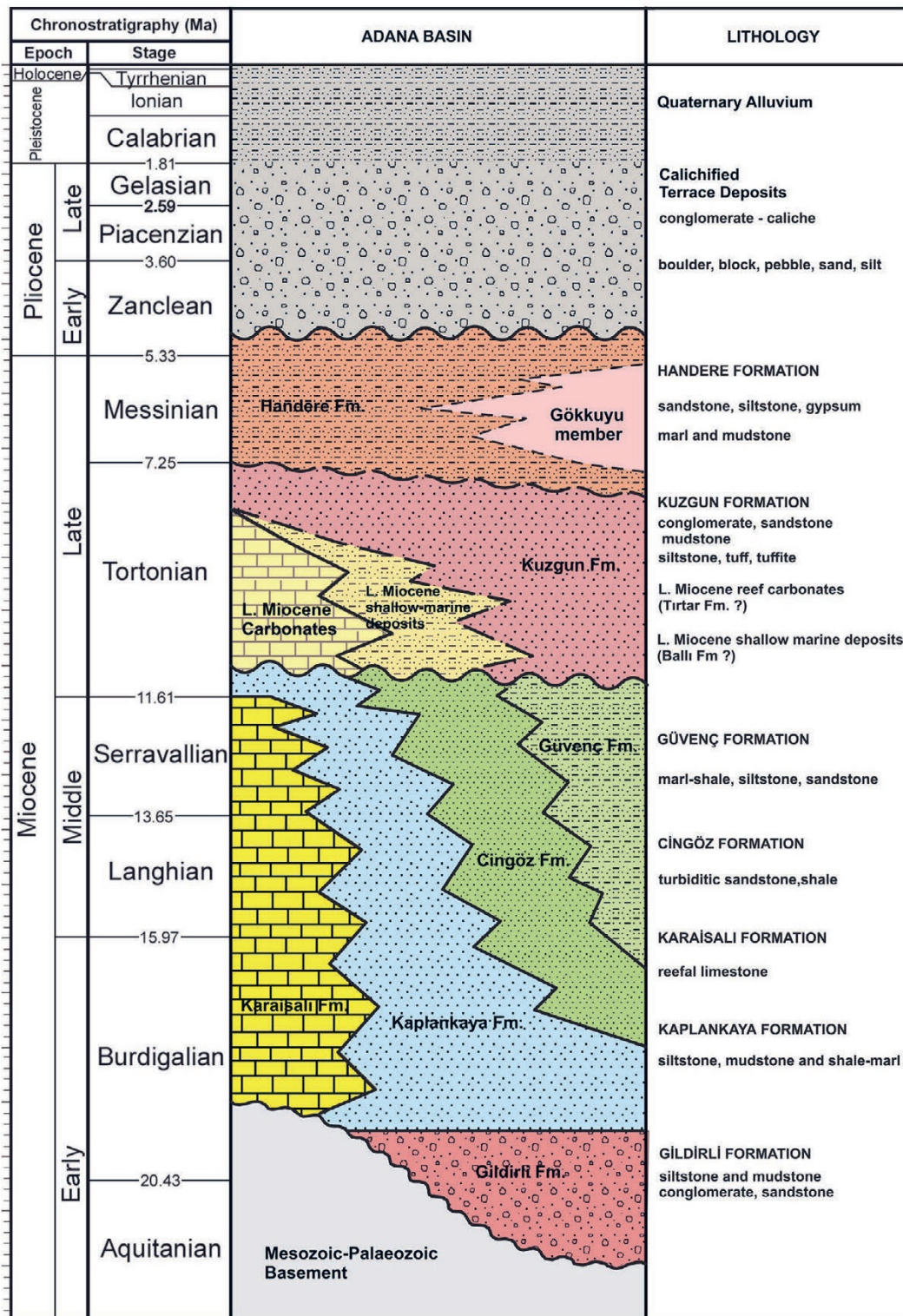


Figure 2. Stratigraphic column showing the relationships of the units in the Adana basin (modified after ILGAR et al., 2013 and ÜNLÜĞENÇ, 1993)

## 2.2. The Kaplankaya and Karaisalı Formations

These two closely related units together represent the Miocene shallow-marine/platform deposits in the basin (ÜNLÜĞENÇ & AKINCI, 2020). The Kaplankaya Formation includes alternations of conglomerates, sandstones, mudstones, shales, and marls. The unit is exposed in the northern part of the Adana Basin around the Arapalı, Gülüşlü, Taşobası, Çokak, Koçmarlı, and Hankaşı villages (Fig. 1). The Kaplankaya Formation was deposited in a shallow marine environment

close to the shore, surrounding the reefal Karaisalı limestone. It transitions into the turbiditic Cingöz Formation in the deeper parts of the basin in the east/northeast of the Karaisalı district and passes into the deeper marine Güvenç Formation in the south (Fig. 2). The Kaplankaya Formation unconformably overlies the Gıldırlı Formation, Mesozoic–Palaeozoic basement rocks, and the Oligocene Karsantı Formation. The sedimentary environments represented in this unit include an alluvial fan type setting at the lower levels, passing upward

into a fan delta and shallow marine environment. The fossil evidence indicates that the Kaplankaya Formation was deposited during lower–middle Miocene time (ÜNLÜGENÇ, 1993). The Karaisalı Formation comprises massive and thick-bedded reefal carbonates and is exposed along the northern margin of the Adana Basin, especially around the western part of the Karaisalı district. The unit includes corals, coralline algae, molluscs, echinoderms, foraminifera, and minor bryozoans. The carbonate rocks of the unit were deposited on pre-Miocene topographical highs and are represented by coral wackestone, packstone, and benthic foraminiferal packstone subfacies that form the talus deposits on the submarine fore-reef slopes (YALÇIN & GÖRÜR, 1984). TARAF et al. (2013) identified three facies and nine microfacies pointing to different parts of the reef, especially based on the lithology and fossil content of the unit. The carbonates of the Karaisalı Formation are seen in the form of both barrier and patch reefs and microfossil determinations have been reported to indicate a Burdigalian–Langhian time interval of deposition (ÜNLÜGENÇ, 1993). According to ILGAR et al. (2013), the Cingöz and Güvenç formations are laterally transitional and conformably overlie the Kaplankaya Fm (Fig. 2). The Karaisalı and closely associated (interfingering) clastic Kaplankaya Formations rest directly on the Palaeozoic units and the Gildirli Formation with an angular unconformity. In the NW of the Karaisalı district, the Kaplankaya Formation unconformably overlain by a thin layer of reef carbonates.

### 2.3. The Cingöz Formation

The Cingöz Formation is a turbiditic submarine-fan unit that crops out widely in the northern part of the Adana Basin, around the Cingöz, Kuşçusofulu, Eğlence, Nergizlik, and Eğner villages. The unit forms two large submarine fans in the east of the Karaisalı district, a major one to the east and a smaller one to the west. The Cingöz Formation comprises alternations of sandstones, pebbly sandstones, shales, mudstones, and marls. The sandstones exhibit both lenticular and parallel bedding, erosional bases and include slumps and abundant sole marks. Additionally, the sandstones show a partial “Bouma Sequence”. Pebbly sandstones and occasional conglomerates are observed to have been deposited as submarine channel fills. The grain size of the clastics in the unit decreases towards the south indicating a southward transport. The Cingöz Formation rests on the Gildirli and Kaplankaya Formations with a locally erosive contact (ÜNLÜGENÇ & ŞAFK, 1992). The western submarine fan system of the Cingöz Formation has been supplied through a major channel formed by a palaeo-valley (DERMAN & GÜRBÜZ, 2007). According to their fossil determinations, NAZİK & GÜRBÜZ (1992) documented that the Cingöz Formation was deposited during the late Burdigalian–Serravallian interval.

### 2.4. The Güvenç Formation

The Güvenç Formation is characterized by the alternations of shales, mudstones, siltstones, marls, and fine-grained sandstones. The fine-grained clastic rocks of the unit are bluish to greenish-grey in colour, thinly parallel bedded, with convolute lamination. They are also carbonaceous and include abundant microfauna. The Güvenç Formation is exposed

mainly in the eastern and south-eastern parts of the Karaisalı district, around the Güvenç, Sevinçli, and Çatalan villages (Fig. 1). ŞAFK & ÜNLÜGENÇ (1992) reported that the Kaplankaya Formation conformably overlies the Gildirli Formation and grades vertically and laterally into the Karaisalı Formation limestones (Fig. 2). Defining the boundary between the Cingöz and Güvenç formations is challenging due to the gradual deepening of the depositional environment (ÜNLÜGENÇ, 1993). The Güvenç Formation represents a shoaling upward sequence toward the south and passes upward into the Kuzgun Formation with a low degree angular discordance that characterises the beginning of the regressive cycle in the basin.

### 2.5. Late Miocene Carbonates

Late Miocene reefal carbonate deposits were described by ATABEY et al. (2000) as the Tirtar Formation in the adjacent westerly Mut Basin. The units are generally considered to be the slightly younger (late Miocene) counterparts of the early-middle Miocene Karaisalı and Kaplankaya formations (Early–Middle Miocene) in the Adana Basin. In the Central Taurus Miocene basins adjacent to the Adana Basin, the late Miocene aged Tirtar and Ballı formations unconformably overlie the middle Miocene sediments (ATABEY et al., 2000). These younger carbonates consist of reefal limestones similar to the underlying Karaisalı Formation. The Ballı formation, like the Kaplankaya Formation in the Adana Basin, consists of fine-grained clastics, marl and other semi-pelagic and pelagic sediments deposited around and beyond the reef and platform carbonates (ATABEY et al., 2000). These units were first presented in the stratigraphy of the Adana Basin by ILGAR et al. (2013) but was not mapped in detail (Fig. 2). The authors suggest that the transgression (relative sea-level rise) initiated a second generation of reef formation with shallow-marine sedimentation along the basin margin in the early Tortonian, the late Miocene reef carbonates, deposited on the older reefal limestones of the Karaisalı Formation. Similar young reefal carbonate formations occur as patches in the southern parts of Adana city centre, around the neighbourhoods of Köklüce and Alihocalı, where they are being exploited as limestone quarries for construction and cement production.

### 2.6. The Kuzgun Formation

Fine-grained clastic sediments of the Güvenç Formation are unconformably overlain by coarser-grained deposits of the Kuzgun Formation. Although, the boundary is discordant, the exact duration of the hiatus is not well defined. The Kuzgun Formation mainly outcrops around the Kuzgun, Salbaş, Karakuyu, and Kaşoba villages (NW Adana). Three facies types were differentiated in the unit (ÜNLÜGENÇ, 1993). At the base, the formation begins with channelized conglomerates, followed by cross-bedded sandy conglomerates, sandstones, and mudstones rich in oysters and shells, which are referred to as the Kuzgun Member. This member represents the characteristics of meandering river and beach deposits and passes upwards into flood plain facies (ÜNLÜGENÇ, 1993). A tuffite-dominated volcanoclastic-marl-shale alternating sequence located at the top of this member is known as the Salbaş Tuffite member. In their study on these tuffites, ŞAFK et al. (2021) determined that based on the biostratigraphic

findings, the environment was lagoonal, transitioning to shallower marine conditions with a deepening trend upwards. Located at the top of the formation, the Memiřli member rests stratigraphically on the Salbař Tuffite member and consists of thickening and coarsening upward sandy-silty sequences characterising deltaic facies. The Kuzgun Formation transitionally passes upward into the Handere Formation.

## 2.7. The Handere Formation

The youngest Neogene unit of the Adana Basin, the Handere Formation, transitionally overlies the Memiřli member of the Kuzgun Formation in the southernmost part of the basin. The unit crops out along an approximately east-west trend in the northern parts of the Adana city centre and is discordantly overlain by Quaternary terrace-caliche deposits. The Handere Formation consists of sandstones, mudstones, marls, and conglomerates of fluvial, shallow marine, and lagoonal character (ÜNLÜGENÇ, 1993). Although cross-bedded and channelised conglomeratic deposits, (mainly located at the base levels) are indicative of a fluvial origin, GÜRBÜZ (1985) reported that the conglomeratic sequences exposed in the east of the Seyhan Dam include some shallow marine intercalations. These sandy and conglomeratic deposits are succeeded by sandy-silty sediments and then pass upwards into thick, fossiliferous carbonaceous mudstone deposits. Towards the top of the unit these fine-grained clastics are succeeded by less well cemented sandstones and siltstones including gypsiferous lenses known as the Gökkuyu Gypsum member (Fig. 2).

## 3. METHODOLOGY

Seawater isotope composition is uniform across modern oceans due to the relatively long residence time of strontium ( $1.5 \times 10^6$  years) (MCARTHUR, 1994; MCARTHUR et al., 2012; KUZNETSOV et al., 2012) and the short mixing time of water masses (JONES & JENKYN, 2001). Therefore, the Sr isotope ratio ( $^{87}\text{Sr}/^{86}\text{Sr}$ ) of ancient seawater can be constructed from well-preserved authigenic minerals and used for studying the stratigraphy of marine sediments. The variation in the isotope composition of Sr may also be a marker of diagenetic alteration and can be used to evaluate fluid-rock interactions of marine rocks (ULLMAN et al., 2013).

The Sr contents of seawater vary due to several factors: (a) the amount of high  $^{87}\text{Sr}/^{86}\text{Sr}$  terrigenous detritus entering the ocean from continental weathering relative to the low  $^{87}\text{Sr}/^{86}\text{Sr}$  contents of oceanic crust due to hydrothermal exchange at mid-ocean ridges; and (b) the seafloor dissolution of carbonates acting as a buffer by adding Sr at a similar ratio to seawater (OSLICK et al., 1994; MCARTHUR, 1994). The diagenetic carbonate flux is an order of magnitude less than the erosional and hydrothermal fluxes. Much effort has been directed at constraining the shape of the Sr ratio curve over time (MILLER et al., 1991; OSLICK et al., 1994; GLEASON et al., 2002). Thus, the highest temporal resolution is obtained for portions of the seawater curve that exhibit the highest rate of change in the  $^{87}\text{Sr}/^{86}\text{Sr}$  ratio as a function of time. There was an acceptable rate of change throughout the late Miocene. In the Mediterranean region, the Sr isotopic methods failed because the basins were constrained and the strontium isotope

ratio was affected by a change in the freshwater to seawater ratio, resulting in anomalous  $^{87}\text{Sr}/^{86}\text{Sr}$  ratios in the Messinian period (FLECKER & ELLAM, 2006).

Strontium is derived from biogenic carbonate, which is the major sink of Sr in the oceans (BRASS, 1976; HODELL, 1994). Organisms that form carbonate shells do not fractionate Sr isotopes. Therefore, it is reasonable to assume that the  $^{87}\text{Sr}/^{86}\text{Sr}$  ratio in biogenic carbonate reflects the seawater composition at the time of precipitation. For strontium analysis, composite samples of benthic foraminifera, gastropods, marls, and carbonatic clastics were selected from the specific sites of the Adana Basin (Fig. 1). A leaching process was carried out in order to remove the residues related to contamination after the samples were ground into rock powder. This process was performed using diluted  $\text{HNO}_3$  in an ultrasonic bath to eliminate surface contamination and detrital impurities prior to geochemical studies. Three repetitive ultrasonic baths with double distilled water were used to clean the gastropod/ostraea tests. Strontium isotope analyses ( $^{87}\text{Sr}/^{86}\text{Sr}$ ) were performed at the Radiogenic Isotope Laboratory of Middle East Technical University, Ankara, Turkey. Chemical treatment and column chemistry were performed in a 100-class clean laboratory with ultrapure chemical agents. Powdered rock samples (approximately 120 mg) were leached with 4 ml of 14 N  $\text{HNO}_3$  for 4 days on the hot plate ( $>100^\circ\text{C}$ ). These samples were dried and dissolved overnight in 4 ml 6 N HCl on the hot plate. Afterward, samples were re-dried, then dissolved in 1 ml 2.5 N HCl for Sr chromatography. Strontium was separated from other elements in 2 ml volume BioRad AG50 W-X8 (100–200 mesh) resin in Teflon columns in a 2.5 N HCl medium. Strontium was loaded on single Re filaments with 0.005 N  $\text{H}_3\text{PO}_4$  and Ta activator to improve efficiency.  $^{87}\text{Sr}/^{86}\text{Sr}$  ratios are normalized with  $^{86}\text{Sr}/^{88}\text{Sr} = 0.1194$ . Measurements were made by multicollection using the Triton Thermal Ionization Mass Spectrometer (Thermo-Fisher). During the analyses the Sr NBS 987 standard was measured as  $0.710260 \pm 10$  ( $n = 3$ ) and no bias correction was applied on the measured Sr isotope data. The analytical uncertainties were determined to be at the 2 sigma level. Further details of the isotope methods that followed at the laboratory are described by KÖKSAL et al. (2019).

Since diagenetic alteration could potentially alter the original Sr composition in the rocks, thin sections were prepared from the collected hand samples and examined in detail under a polarizing microscope to determine whether they had undergone any alteration. An elementary palaeontological study was carried out to test the  $^{87}\text{Sr}/^{86}\text{Sr}$  age data for the Cingöz and Güvenç formations, which were thought to be affected by diagenetic alteration. For this purpose, some of the collected rock samples of these units crushed and treated with hot water and 15% diluted hydrogen peroxide ( $\text{H}_2\text{O}_2$ ) in glass beakers for at least 24 hours. The disaggregated residues later were subsequently washed through 0.60, 0.120, and 0.230 mm mesh sieves and placed in sample bags after oven drying. The microfossils were separated from grains under the microscope and placed on slides for taxonomic identification. SEM photomicrographs of the identified fossils were captured using the FEI Quanta 650 in the Central Research Laboratory of Çukurova University.

Sedimentological logs were prepared from the Sr sampling sites to reveal the general sedimentological characteristics of the unit at that level.

Ca, Fe, Mg and Mn concentrations used in diagenetic alteration assessment were determined in the Çukurova University Geological Engineering Department Geochemistry Laboratory with Wet Chemical methods and using Atomic Absorption Spectrometer (Perkin Elmer Analyst 700). Sr concentration measurement was performed in Çukurova University's Central Laboratory using an AAS (Perkin Elmer PinAAcle 900T).

#### 4. ASSESSMENT OF DIAGENETIC ALTERATION

Diagenesis of sedimentary rocks may lead to decreased concentrations of Sr and increased Mn and Fe (e.g., BRAND & VEIZER, 1980; VEIZER, 1983; AL-AASM & VEIZER, 1986). Marine carbonates reflect the strontium isotopic composition of ambient seawater, which allows determination of the time of mineral formation if not affected by advanced diagenesis (HOWARTH & MCARTHUR, 1997; MCARTHUR et al., 2001; MCARTHUR et al., 2012). Although the  $^{87}\text{Sr}/^{86}\text{Sr}$  compositions are preferably measured on fossil shells such as oysters and pectinids because of their high preservation potential and reliability (SCASSO et al., 2001; SCHNEIDER et al., 2009; BRANDANO & POLICICCHIO, 2012; VESCOGNI et al., 2014; ARGENTINO et al., 2017), sufficient quantities of fossil shells for  $^{87}\text{Sr}/^{86}\text{Sr}$  analysis may not be available in all cases (e.g. for units dominated by planktonic species). In addition, it is not possible to extract tests from strongly cemented reef carbonates. Nevertheless, we have ensured through widely used petrographic methods such as thin sections and SEM images that it has not been subjected to significant diagenetic alterations. In this study, oyster and gastropod fossil shells were used in one of the six units (Kuzgun Formation) for  $^{87}\text{Sr}/^{86}\text{Sr}$  analysis, however, this was not possible for the other units due to insufficient fossilised shell content for comprehensive analysis (Tables 1, 2). For this reason, geochemical, petrographic evaluation of thin sections and SEM images were used to assess bulk samples, and any effects of diagenetic alteration in potentially altered samples will be considered in subsequent geological evaluations.

##### 4.1. Thin-section examination

Carbonate rocks are exposed to especially meteoric and groundwater during diagenesis and therefore they can show alteration. The investigated carbonate rocks in the Adana Basin are Miocene in age and have been uplifted (between 150-600 m) by gradual regression (ÜNLÜGENÇ, 1993; ÜNLÜGENÇ & AKINCI, 2020) since this period, and it is unlikely that they have undergone metasomatism due to deep burial. In this case, carbonate material could be dissolved by the acidic waters and secondary carbonate or ferrous/silica mineralization can be present along micro-cracks or pores. In addition, secondary dolomitization with magnesium enrichment can also be seen. These alteration features can be determined by petrographic examinations made on thin sections under a polarizing microscope. Thus, carbonate rocks that lack abundant secondary crystallisation, dolomitization, or iron enrichment, and have preserved their original fossil and textural character-

Table 1. Geochemical analysis results (trace element concentrations) of the studied rock samples.

Unit	Sample Code	Sample Type	$^{87}\text{Sr}/^{86}\text{Sr}$	% Ca	% Mg	Fe (ppm)	Mn (ppm)	Sr (ppm)	Mg/Ca	Fe/Sr	Mn/Sr
Kuzgun Fm.	Kz-1	Ostrea shell	0.708967	21.31	1.55	1090	175	751.9	0.073	1.45	0.23
	Kz-2	Ostrea shell	0.709172	33.89	1.3	680	2349	448.8	0.038	1.52	5.23
	Kz-3	Gastropod shell	0.70916	35.86	0.81	380	1620	467.9	0.023	0.81	3.46
L. Miocene Reef Carbonates	T-2	Bulk rock – Limestone	0.708962	37.29	1.18	1200	110.8	508.9	0.032	2.36	0.22
Güvenç Fm.	G-1	Clayey Limestone	0.708646	9.48	2.63	3130	586.4	279	0.277	11.22	2.10
	G-2	Calcareous detritic	0.708292	8.51	3.32	3600	652.5	231	0.390	15.59	2.82
	G-3	Calcareous detritic	0.708149	7.93	3.15	3880	685.2	246.9	0.397	15.71	2.78
Cingöz Fm.	C-1	Calcareous detritic	0.708848	8.19	2.52	3340	633.7	229	0.308	14.59	2.77
	C-2	Calcareous detritic	0.70825	6.16	1.66	3570	378.3	117	0.269	30.52	3.23
	C-3	Clayey Limestone	0.708236	17.85	3.75	2550	365.4	315.4	0.210	8.08	1.16
Kaplankaya/Karaisalı Fm.	K-2	Bulk rock – Limestone	0.708909	29.6	1.99	1040	202.6	847.8	0.067	1.23	0.24
	K-4	Bulk rock – Limestone	0.708954	19.64	2.79	2230	255.4	480	0.142	4.65	0.53

**Table 2.**  $^{87}\text{Sr}/^{86}\text{Sr}$  isotopic results and corresponding age ranges of the analysed samples with literature sources. 3 of 15 samples were returned without results from the laboratory. Standard errors belong to the last one or two digits (e.g.:  $\pm 0.000006$  or  $\pm 0.000018$ ).  $^{87}\text{Sr}/^{86}\text{Sr}$  results corrected for the NBS 987 standard and were measured as  $0.710260 \pm 10$  ( $n=3$ ).

Unit	Sample Code	Sample Type	$^{87}\text{Sr}/^{86}\text{Sr}$	std error*	$^{87}\text{Sr}/^{86}\text{Sr}$ age range (ma)/stage	Literature Age (Paleontologic)
Handere Fm.	H-1	Bulk rock – Marl	No Result		NA	Mersinian – Pliocene (SCHMIDT, 1961, GÜRBÜZ 1985, ÜNLÜĞENÇ, 1993).
	H-2	Bulk rock – Marl	No Result		NA	
Kuzgun Fm.	Kz-1	Ostrea shell	0.708967	$\pm 10$	7.4 $\pm$ 2 ma / Tortonian – Messinian	Late Miocene (SCHMIDT, 1961; İLKER, 1975; YALÇIN & GÖRÜR 1984); Tortonian (YETİŞ, 1988, ÖGRÜNÇ, 2001)
	Kz-2	Ostrea shell	0.709172	$\pm 14$	1 $\pm$ 0.5 ma / Pleistocene	
	Kz-3	Gastropod shell	0.70916	$\pm 16$	1.3 $\pm$ 0.7 ma / Pliocene – Pleistocene	
L. Miocene Reef Carbonates	T-1	Bulk rock – Limestone	No Result		NA	L. Miocene/Tortonian (ILGAR et al., 2013)
	T-2	Bulk rock – Limestone	0.708962	$\pm 12$	7.3 $\pm$ 2.1 ma / Tortonian – Messinian	
Güvenç Fm.	G-1	Clayey Limestone	0.708646	$\pm 15$	16.9 $\pm$ 0.9 ma / Burdigalian – Langhian	Burdigalian – Langhian (YETİŞ, 1994) Serravallian (NAZİK & GÜRBÜZ, 1992); Langhian – Serravallian (NAZİK, 1983, This study)
	G-2	Calcareous detritic	0.708292	$\pm 15$	22 $\pm$ 1.2 ma / Aquitanian	
	G-3	Calcareous detritic	0.708149	$\pm 9$	25 $\pm$ 0.6 ma / Chattian	
Cingöz Fm.	C-1	Calcareous detritic	0.708848	$\pm 15$	12 $\pm$ 2.1 ma / Serravallian – Tortonian	Late Burdigalian – early Serravallian (NAZİK & GÜRBÜZ, 1992); late Burdigalian – Serravallian (ŞAFAK, 1993), Burdigalian – Serravallian (This study)
	C-2	Calcareous detritic	0.70825	$\pm 7$	23 $\pm$ 1.3 ma / Chattian – Aquitanian	
	C-3	Clayey Limestone	0.708236	$\pm 10$	22.8 $\pm$ 1.5 ma / Chattian – Aquitanian	
Kaplankaya/Karaisalı Fm.	K-2	Bulk rock – Marl	0.708909	$\pm 16$	10 $\pm$ 2.5 ma / Serravallian – Tortonian	Lower-middle Miocene* (ÜNLÜĞENÇ, 1993), L. Burdigalian – Serravallian (SINACI, 2010)
	K-4	Bulk rock – Marl	0.708954	$\pm 15$	9.5 $\pm$ 2.4 ma / Serravallian – Tortonian	

istics, are considered to have undergone minimal diagenetic alteration.

The carbonate rocks compiled for Sr isotope analysis from the Late Miocene carbonates (Figs. 3a-c) show a boundstone texture expressing the reefal facies and dominated by algae. The rock also contains small amounts of microfossils and is cemented by sparite. It does not show any significant recrystallization in thin section examination, and it largely preserves its original texture. The samples collected from the Kaplankaya Fm. contain abundant microfossils (mostly foraminifera) and include a small amount of (5-10%) detrital fragments in a relatively fine-crystalline sparry calcite cement (packstone) (Figs. 3d-f). The rock lacks cracks/pores, exhibits no recrystallization, and preserves its original sedimentary texture without showing significant signs of alteration.

The sampling for Sr isotope analysis from the Cingöz and Güvenç formations is the most suspicious in terms of diagenetic alteration. Due to the sedimentological characteristics of these units (deep sea/continental slope environment), it is challenging to obtain sufficient shell material or primary pure carbonate rock samples. However, a challenge was undertaken by compiling and analysing the marl samples with the highest possible chemical carbonate content. Due to the nature of the rocks being easily fragmented, comminution occurred during the preparation of thin sections. Therefore, thin sections were prepared using resin. However, in thin section examination, both the Cingöz Formation (Fig. 3g-i) and the Güvenç Formation (Fig. 3j-l) proved to be rich in detritus (15-25%) and show significant alteration traces. This situation can also be seen in SEM images of the fossil shells (Fig. 4) and geochemical analysis (high Fe and Mn concentrations). For this reason, the effect of diagenetic alteration was considered for these two units and performed a basic biostratigraphic study to test obtained  $^{87}\text{Sr}/^{86}\text{Sr}$  ages for these units.

Only oyster and gastropod shells were used for Sr isotope analysis of the Kuzgun Formation, which has been abundant in the unit. In the preparation of powder samples from shells, first the outer surface of the shell was washed and dried to minimize any potential alteration. A thin section was prepared in order to determine whether there is widespread alteration in the unit (Fig. 3m-o). In the examination, it was observed that the rock is composed of marl (Fig. 3m, n) and carbonate mudstone. No secondary mineralization was encountered, and it does not show any significant alteration traces identified from the images. Although the laboratory couldn't measure the Sr ratio of the Handere Formation, the thin-section images of the samples compiled for the Handere Formation (Figs. 3p-s) were also examined. These samples are partly fossiliferous in a micrite cement, their primary sedimentary features are preserved and they do not bear any significant alteration traces. However, secondary calcite likely affected the strontium composition somehow, since the unit was highly calcified at some levels.

## 4.2. Geochemical Analysis

Several geochemical analysis techniques are available to evaluate the diagenetic effects in sedimentary rocks post-deposition. To assess the degree of post-depositional changes



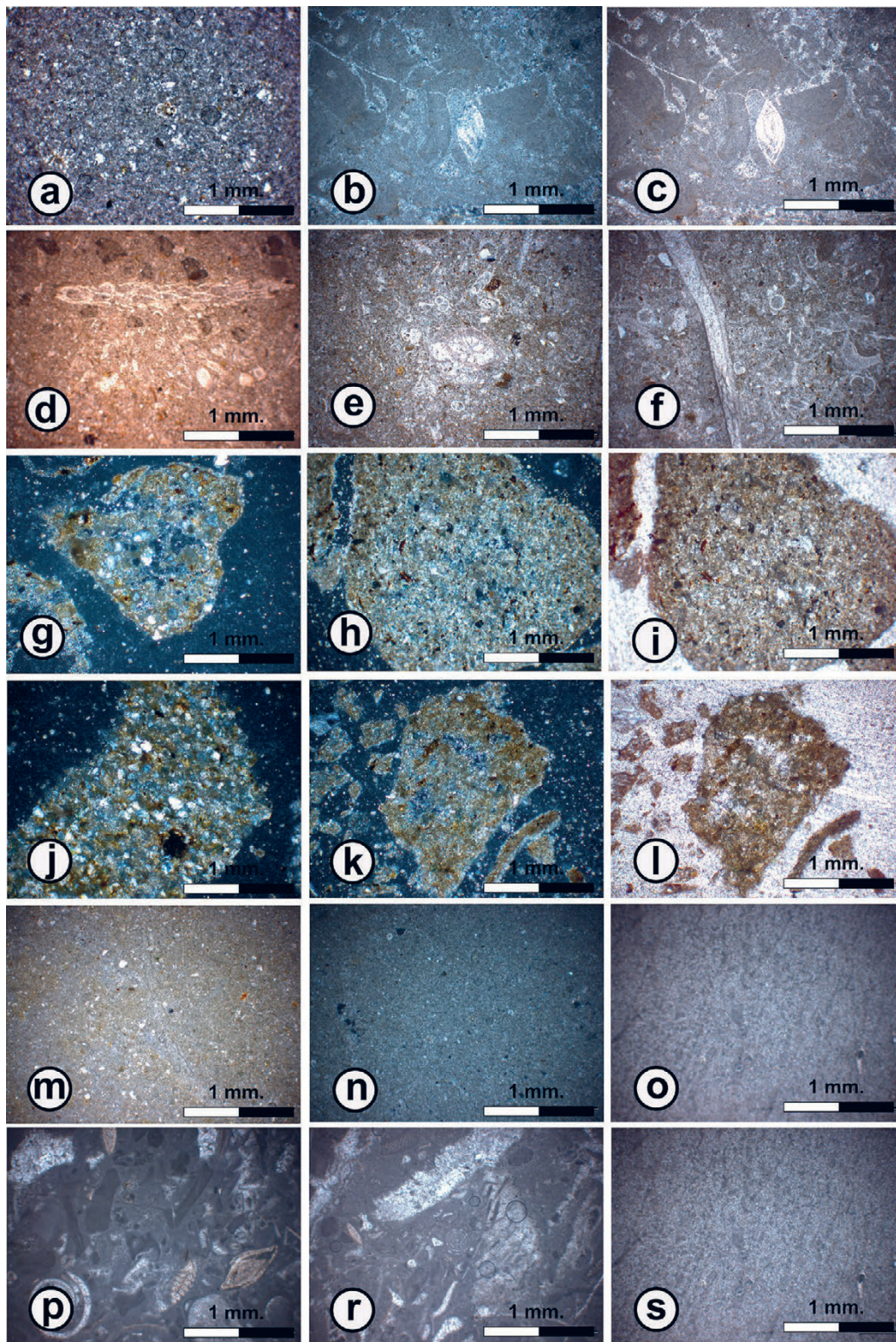


**Figure 3.** Thin-section photomicrographs of bulk-rock samples collected from the field for  $^{87}\text{Sr}/^{86}\text{Sr}$  analysis: a) T-1 (Tirtar Fm.); b-c) T-2 (Tirtar Fm.); d) K-1 (Kaplankaya Fm.); e-f) K-2 (Kaplankaya Fm.); g) C-1 (Cingöz Fm. (prepared in resin)); h-i) C-3 (Cingöz Fm.); j) G-1 (Güvenç Fm. (prepared in resin)), k-l) G-2 (Güvenç Fm.); m) Kz-1 (Kuzgun Fm. (oyster shells used for Sr analysis of Kuzgun Fm.)), n) Kz-2 Kuzgun Fm.; o) Kz-3 (Kuzgun Fm.); p-r) H-1 (Handere Fm.), s) H-2 (Handere Fm.). While the primary diagenetic features seem to be preserved in the Kaplankaya and Karaisalı formations, an excess of clastic material and some diagenetic differentiation can be observed in the Cingöz and Güvenç formations. See text for further explanations.

in carbonate rocks and shells there are several criteria in world practice:  $\text{Mn}/\text{Sr} < 1.5$  and  $\text{Rb}/\text{Sr} < 0.004$  (ASMEROM et al., 1991),  $\text{Mn}/\text{Sr} < 1$ ,  $\text{Rb}/\text{Sr} < 0.002$ , and  $\text{Ca}/\text{Sr} < 1000$  (DERRY et al., 1992),  $\text{Mn}/\text{Sr} < 1.5$  and  $\text{Rb}/\text{Sr} < 0.0005$  (KAUFMAN et al., 1993),  $\text{Mg}/\text{Ca} \leq 0.024$ ,  $\text{Mn}/\text{Sr} \leq 0.2$ ,  $\text{Fe}/\text{Sr} \leq 5.0$  (GOROKHOV et

al., 1995; KUZNETSOV et al., 1997; SEMIKHATOV et al., 1998)  $\text{Mg}/\text{Ca} \leq 0.608$ ,  $\text{Mn}/\text{Sr} \leq 1.2$ ,  $\text{Fe}/\text{Sr} \leq 3.0$  (KUZNETSOV et al., 2003). Table 1 shows the results of the geochemical analysis for the samples with  $^{87}\text{Sr}/^{86}\text{Sr}$  results. In this study, it was evaluated according to KUZNETSOV et al. (2003, 2012),

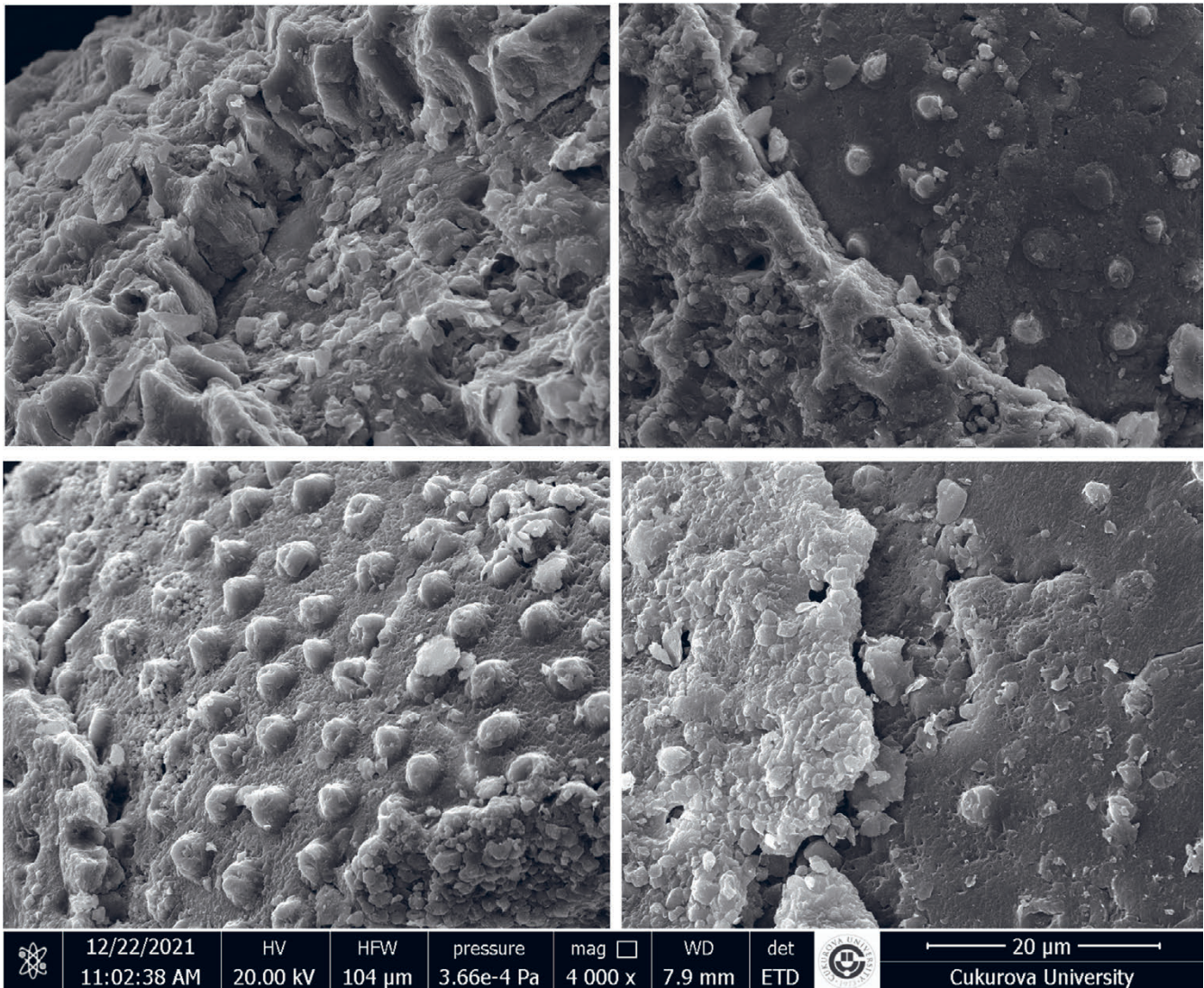


**Figure 4.** SEM images of fossil shells found in the Güvenç (above – *Globigerinoides* sp.) and Cingöz (below – *Orbulina suturalis*) formations. Images indicate that the units considerably affected by alteration marked by significantly etched surfaces; indistinct and fused nacreous tablets. Also secondary calcification can be seen in right bottom image (mag=4000X).

which is one of the most recent studies in the evaluation of diagenetic alteration. According to the results, it is seen that the Mg/Ca and Fe/Sr ratios are very high and may lead to deviations in the  $^{87}\text{Sr}/^{86}\text{Sr}$  ratios of the Güvenç ( $\text{Mg}/\text{Ca}_{\text{max}}=0.39$ ;  $\text{Fe}/\text{Sr}_{\text{max}}=15.71$ ) and Cingöz formations ( $\text{Fe}/\text{Sr}_{\text{max}}=30.52$ ). Exceptionally high Mn concentrations were observed in two samples (Kz-2, Kz-3) from oyster and gastropod shells collected from the Kuzgun Formation (5.23 and 3.46 Mn/Sr, respectively). The geochemical results for other units were within or near acceptable limits. Geochemical analysis results are generally consistent with petrographic and SEM data, suggesting that reliable  $^{87}\text{Sr}/^{86}\text{Sr}$  results are hindered in clastic sediment-dominated units (e.g., Güvenç and Cingöz formations).

Early marine diagenesis is also a critical stage in the diagenetic history of shallow-water carbonate sediments, playing a key role in the transformation of metastable  $\text{CaCO}_3$  polymorphs, e.g. aragonite and high-Mg calcite, into the stable low-Mg calcite (HIGGINS et al., 2018). Although it leaves subtle textural evidence, it significantly impacts primary geochemical signatures, altering stable isotopic ratios and elemental

compositions, which is crucial for interpreting sedimentary records. The chemical evolution of pore fluids during early marine diagenesis and their interaction with sediment composition are central to the mineralogical and geochemical changes observed in ancient shallow-water carbonate sediments. This process may have caused variations in the Sr isotope ratios of units deposited in the basin, particularly during the Upper Miocene and Pliocene.

## 5. RESULTS

The general stratification in the Adana Basin is oriented east-west and dips southward. Sampling and cross-section measurements for strontium analysis and stratigraphic interpretation were carried out approximately along a north-south oriented section within the Adana Basin (Fig. 1). Thus, the results aimed to minimize the influence of lateral facies changes. The selected sections are the locations where the units present their typical characteristics. When collecting Sr samples, there was a general attempt to compile a selection from different stratigraphic levels of the unit. Sedimentary

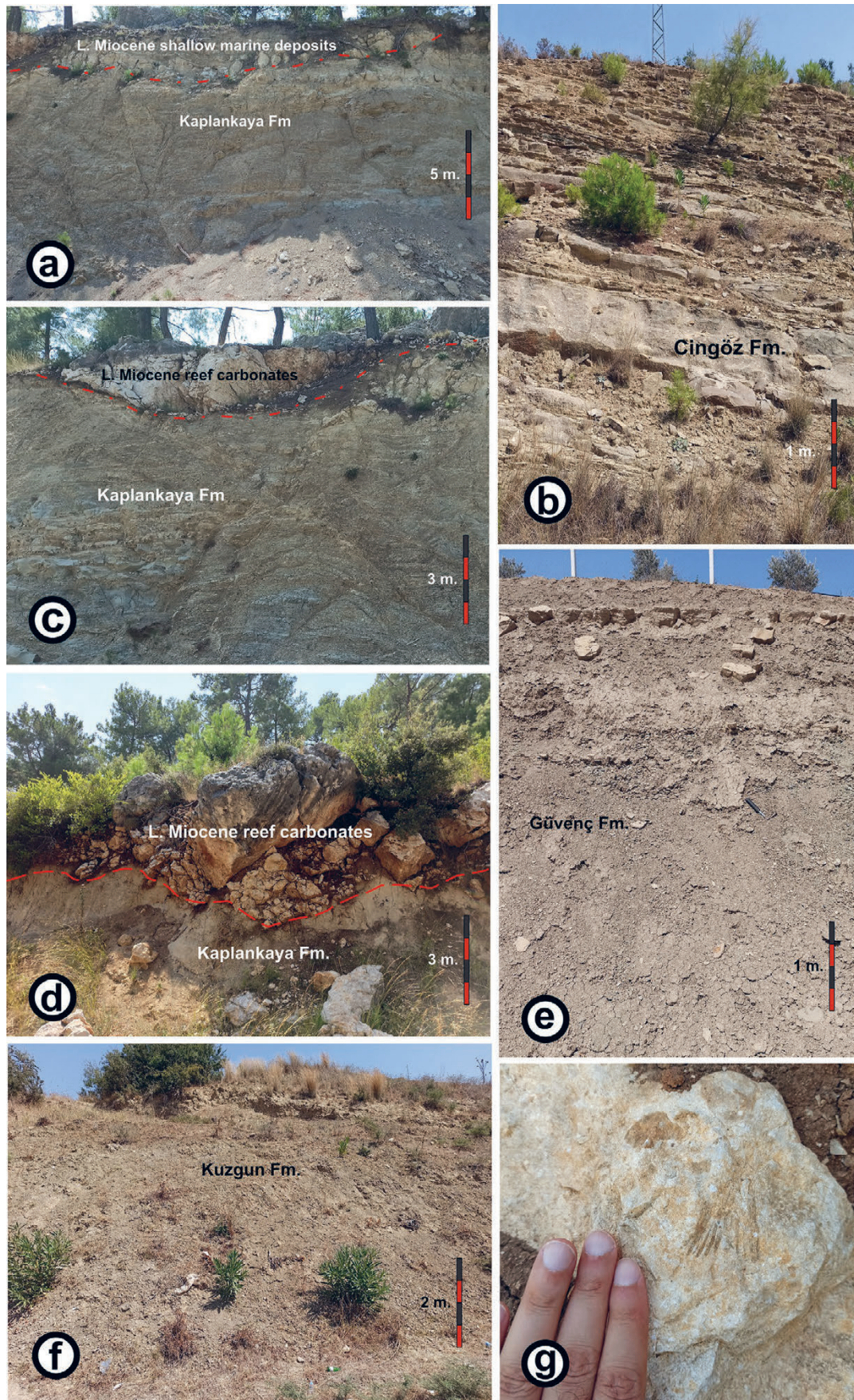


**Figure 5.** Representative outcrop photos of various geological formations showing their in-situ lithological characteristics and stratigraphic relationships in the Adana Basin: a,c,d) Outcrop view of the Kaplankaya and L. Miocene reef carbonates at NE of Karaisalı district (please note that the faulting in Kaplankaya Fm. does not affect the overlying Late Miocene reef carbonates); b) Sandstone-siltstone-shale alternations of the Cingöz Fm. from east of Nergizlik village; e) Road-cut exposure of the Güvenç Fm. near the Güvenç village; f) Outcrop view of the Kuzgun Fm. at the south of Salbaş village; g) Close view of the Late Miocene reef limestones including algae prints.

logs were taken from places where sampling was undertaken and where the characteristics of the units could be clearly observed and are presented separately for each unit below.

### 5.1. The Kaplankaya Formation

Sampling and stratigraphic logging for the Kaplankaya Formation (Figs. 5a, c, d) was undertaken around the village of Gülüşlü (36 S 679674.39 d E/ 4127318.27 m N). Along the section, the Kaplankaya Formation is overlain by the Late Miocene reefal limestones and has a thickness of around 40-50 metres. Field observations were performed along a road cut

between the villages of Karaisalı and Gülüşlü. The unit consists of mudstone and marls containing lamellibranch and conus shells. Three samples (marl) were collected for strontium analysis throughout the investigated section. The two studied sedimentary sections of the Kaplankaya Formation are shown in Figure 6.

The  $^{87}\text{Sr}/^{86}\text{Sr}$  result of one of the three samples of the Kaplankaya Formation could not be successfully obtained in the laboratory. The available  $^{87}\text{Sr}/^{86}\text{Sr}$  age data of the two other samples yielded ages  $9.5 \pm 2.4$  Ma and  $10 \pm 2.5$  Ma coinciding the Serravallian–Tortonian interval (Fig. 7e).

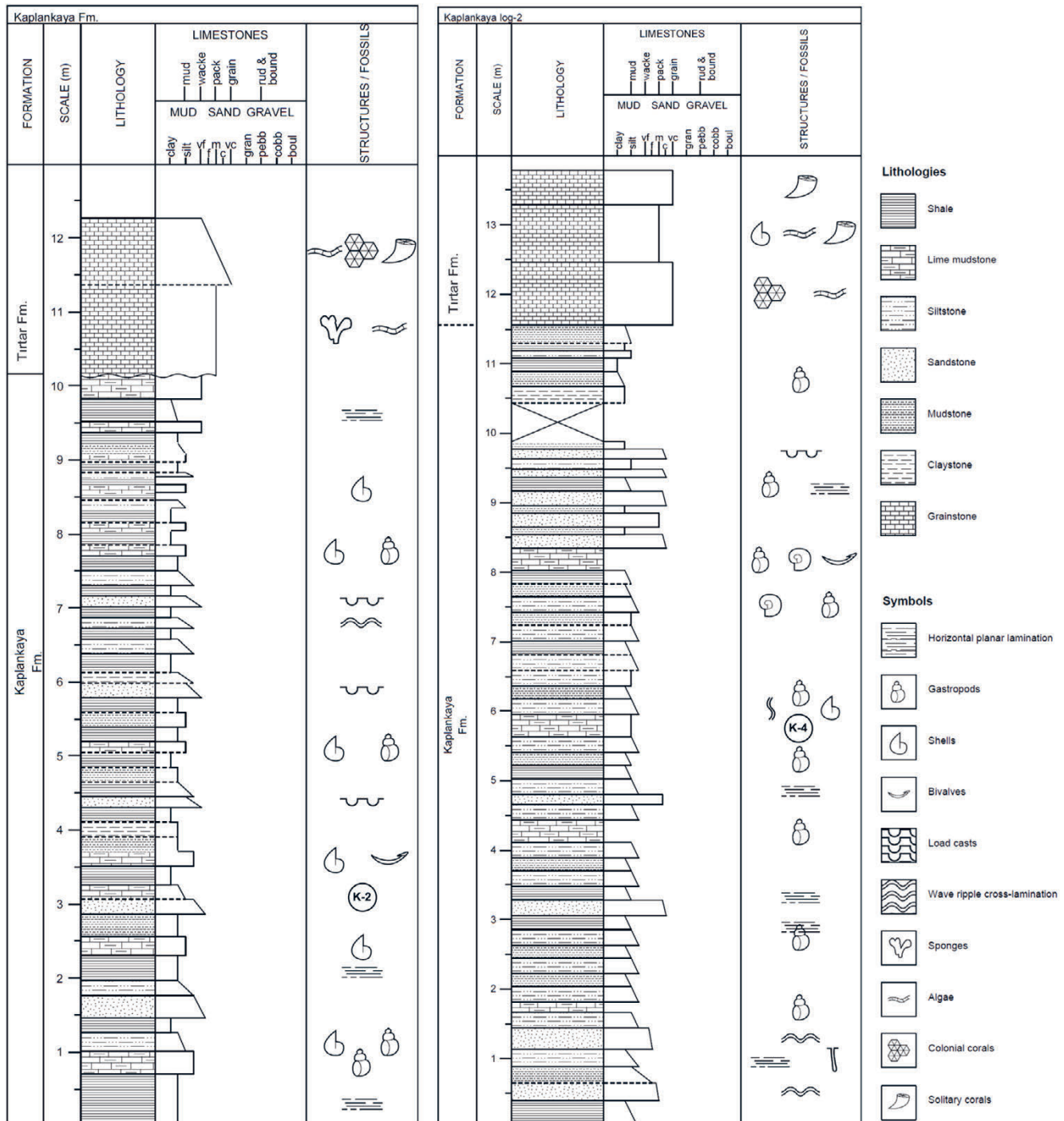


**Figure 6.** Measured sedimentological logs of the Kaplankaya Formation showing the sampling levels (K-2 at left and K-4 at right) for the Sr analysis (see Fig. 1 for locations).

## 5.2. The Cingöz Formation

Stratigraphic logging and sampling for  $^{87}\text{Sr}/^{86}\text{Sr}$  analysis of the Cingöz Formation (Figs. 5b, 8) were performed along with the road cuts on the main road connecting the Karaisalı district centre to the village of Kızıldağ in the northeast (36 S 683730.00 d E / 4131183.00 m N). Samples were collected from three different stratigraphic levels; from the contact with the overlying Güvenç Formation in the south and towards the lowest levels of the unit in the north (C1-bottom, C2-middle, C3-top in Fig. 1). This section constitutes the western submarine fan of the turbiditic Cingöz Formation. A fining upward trend in grain size of the unit comprising alternations of sandstone,

shale, and marl was observed along the section towards the distal zone to the south. The studied sedimentary sections of the Cingöz Formation are presented in Figure 8.

Sr isotope analysis results derived from the samples collected from the Cingöz Formation (Table 2), yielded ages ranging from  $23 \pm 1.3$  Ma (Chattian–Aquitainian) to  $12 \pm 2.1$  Ma (Serravallian–Tortonian) (youngest) (Fig. 7d).

To assess the compatibility of the  $^{87}\text{Sr}/^{86}\text{Sr}$  ages, biostratigraphic dating was applied to samples collected from the Cingöz Formation due to the high clastic content and diagenetic alteration. In the samples compiled from the unit; *Neomonocerotina* cf. *mouliana*, *Cyamocytheridea* sp., *Neomonocerotina*

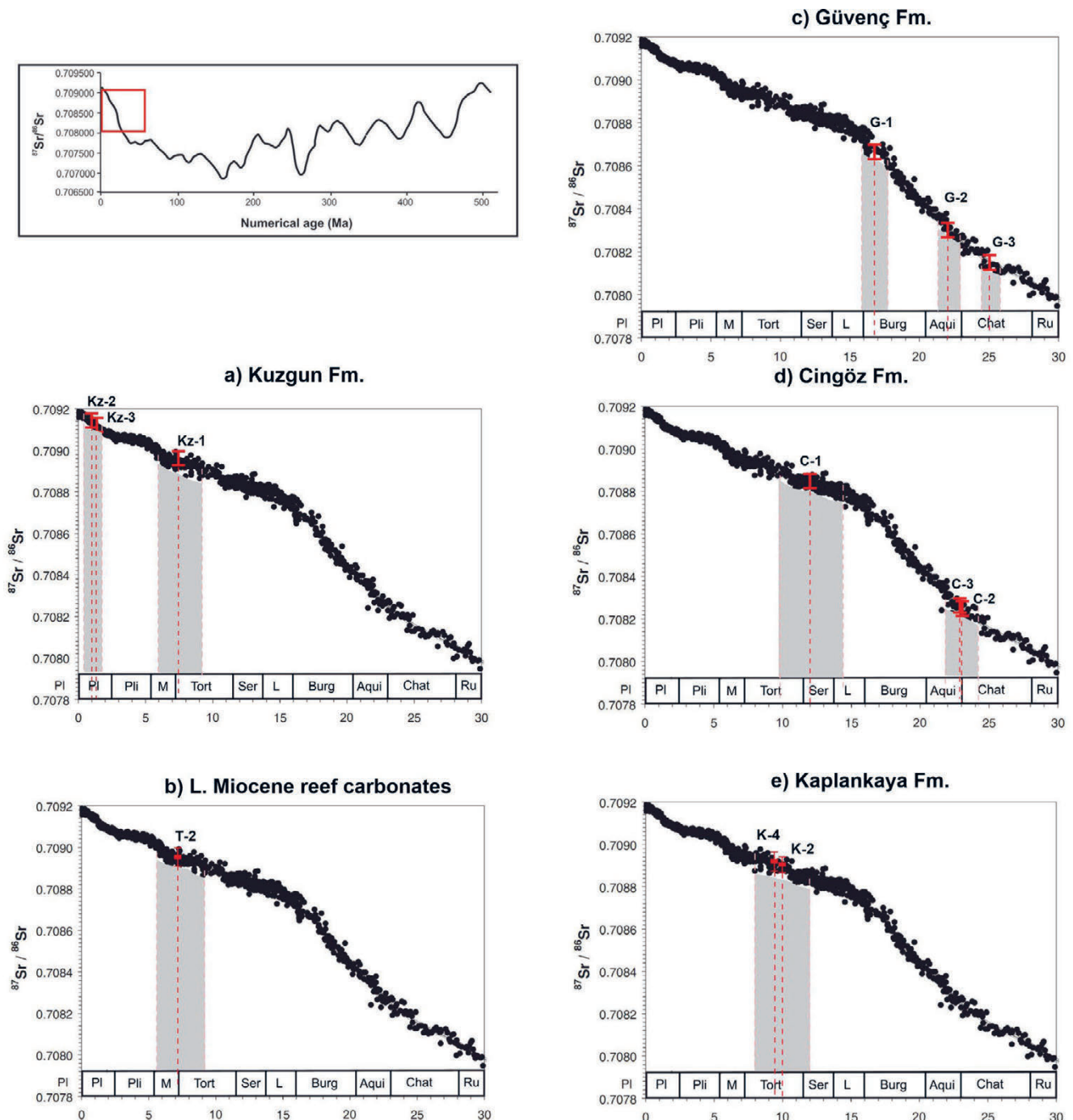


**Figure 7.** Graphs showing the obtained  $^{87}\text{Sr}/^{86}\text{Sr}$  Isotopic age data for all the units studied, presented on the Sr variation curve of MCARTHURET al. (2001); a) Kuzgun Fm.; b) L. Miocene reef carbonates; c) Güvenç Fm.; d) Cingöz Fm.; e) Kaplankaya Fm.

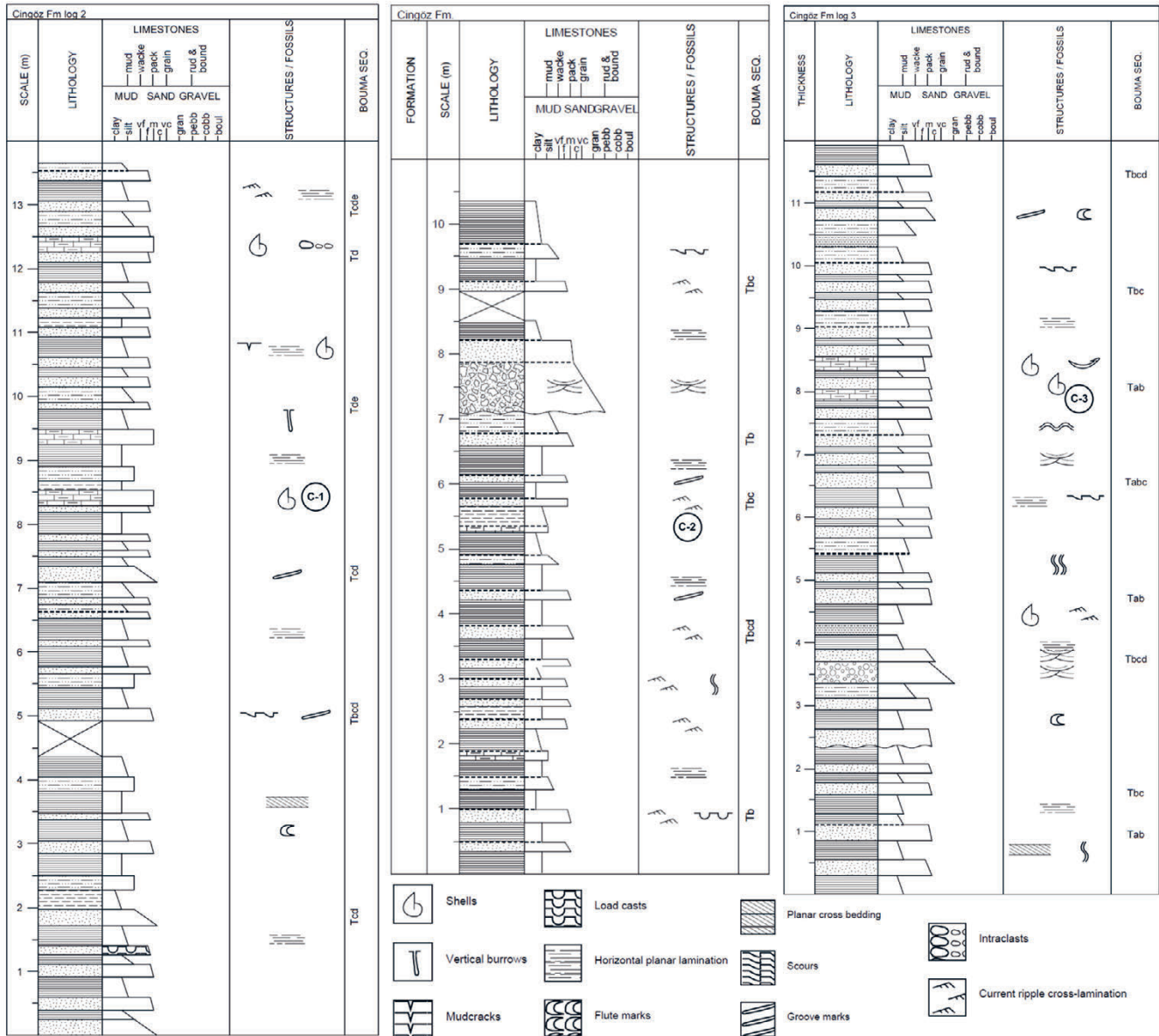


Figure 8. Sedimentological logs measured from the Cingöz Formation showing the levels of the sampling for Sr analysis (see Figure 1 for locations).

sp., *Thalmannia hodgii*, *Tenedocythere prava*, *Acantocythereis hystrix*, *Orbulina suturalis*, *Orbulina universalis*, *Orbulina bilobata*, *Globigerinoides bollii* species were identified which are all indicative of a wide ranging Burdigalian–Serravallian interval (Fig. 9).

### 5.3. The Güvenç Formation

Sampling for strontium isotope analyses and sedimentary logging of the Güvenç Formation (Figs. 5e, 10) were performed along the highway between Güvenç village in the Karaisalı district (location of the type section of the unit), and the village of Kuzgun in the south. Composed of loosely consolidated clay and shale, highly susceptible to erosion, the Güvenç Formation can only be clearly observed in the newly opened road cuts and small galleries along this road. For the strontium isotope analysis, three samples were selected; one near the contact with the underlying Cingöz Formation (G-3) (36 S 683100.00 d E/ 4125229.00 m N), one from the uppermost

levels (36 S 685916.00 d E/ 4113848.00 m N), and one from the middle levels (G-2) (Figs. 1,10).

The recorded  $^{87}\text{Sr}/^{86}\text{Sr}$  ages of the Güvenç Formation are presented in Figure 7 and Table 2. Isotopic analysis of sample G-3, collected near the basal levels of the unit (just above the Cingöz Fm.) is  $25 \pm 0.6$  Ma (Chattian) and the sample collected from the middle level is  $22 \pm 1.2$  Ma (Chattian–Aquitania). The sample G-1, collected from the uppermost levels of the unit, near its contact with the overlying Kuzgun Formation, yielded an age of  $16.9 \pm 0.9$  Ma representing Burdigalian–Langhian interval (Fig. 7c).

Biostratigraphic analysis was conducted to compare with the strontium isotope results, since the Güvenç Formation exhibits a high clastic content, similar to the Cingöz Formation and diagenetic alteration was detected in the thin section examinations. In the samples collected from the unit, *Globigerinoides bollii*, *Globigerinoides subquadratus*, *Globigerinoides* sp., *Globorotalia mayeri*, *Globigerinella obesa*, *Globigerinoides trilobus*, *Globigerinoides* cf. *Sacculifer*, *Globiquadrana*

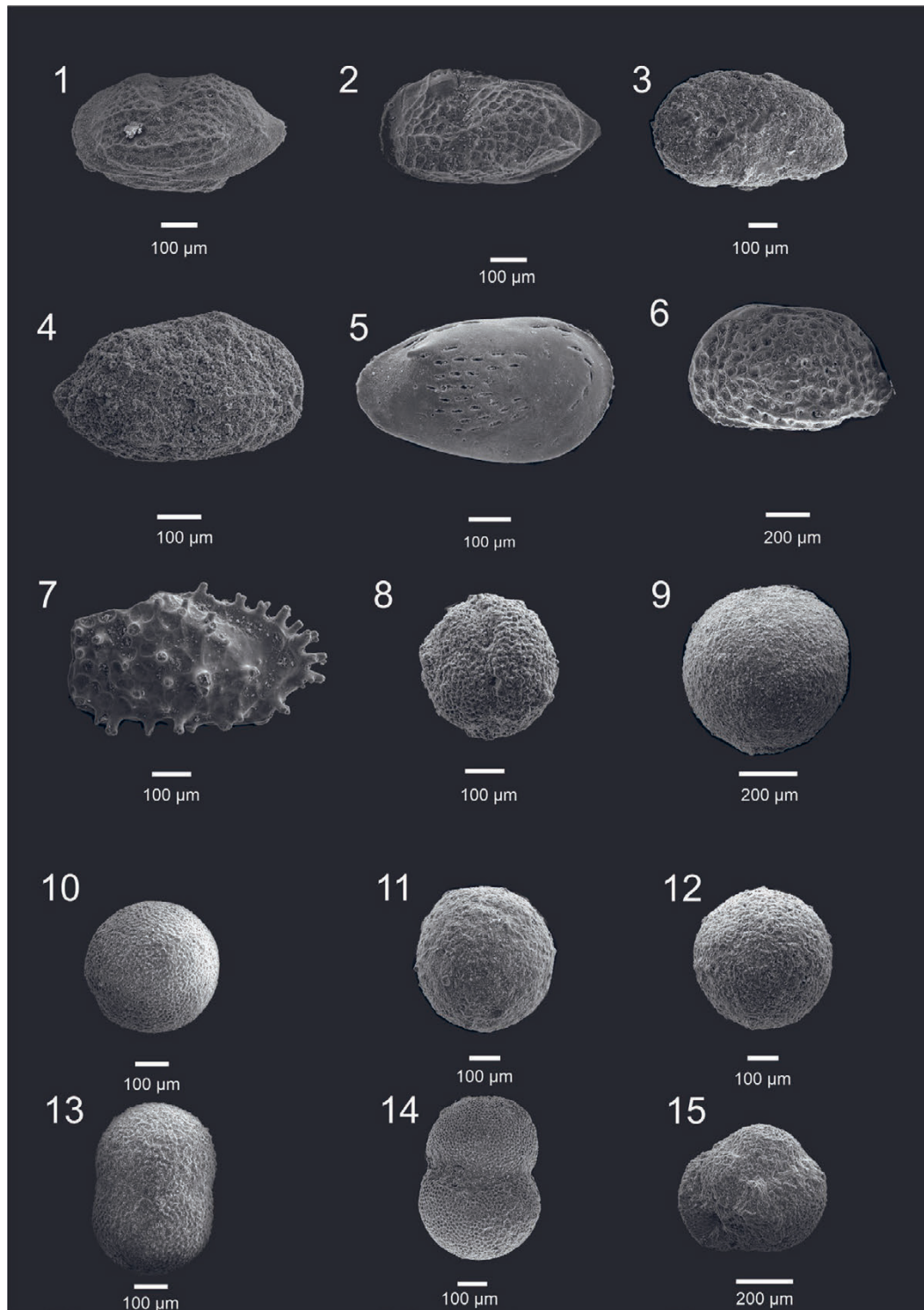


**Figure 9.** SEM images of the micro-fauna identified in the Cingöz formation. 1 – *Neomonoceratina cf. mouliana* (shell, left external view); 2 – *Neomonoceratina cf. mouliana* (shell, left external view); 3 – *Cyamocytheridea* sp. (shell, left external view); 4 – *Neomonoceratina* sp. (shell, right external view); 5 – *Thalmannia hodgii* (right carapace, external view); 6 – *Tenedocythere prava* (left carapace, external view); 7 – *Acantocythereis hystrix* (right carapace, external view); 8 – *Orbulina suturalis*; 9 – *Orbulina suturalis*; 10 – *Orbulina suturalis*; 11 – *Orbulina universa*; 12 – *Orbulina universa*; 13 – *Orbulina bilobata*; 14 – *Orbulina bilobata*; 15 – *Globigerinoides bollii*.

*dehiscensis* and *Sphaeroidinellopsis* sp. species were determined which are all indicative of the Langhian–Serravallian interval (Fig. 11).

#### 5.4. The Late Miocene Reef Carbonates

Given the younger age of the sampled reef carbonate rocks in the vicinity of Güllüşlü village (NW Karaisalı – 36°S 679945.00

E/4127388.00 N) (Fig. 1), they were considered and classified as “Late Miocene reef carbonates”. In this region, the reef carbonates are observed superimposed on the Kaplankaya Formation (Figs. 5a, c, d, g). The stratigraphic log measured from the sampling site reveals that the approximately 6 metre-thick, pale yellow to beige coloured neritic (reefal) carbonate rocks overlie the clastic sediments of the Kaplankaya

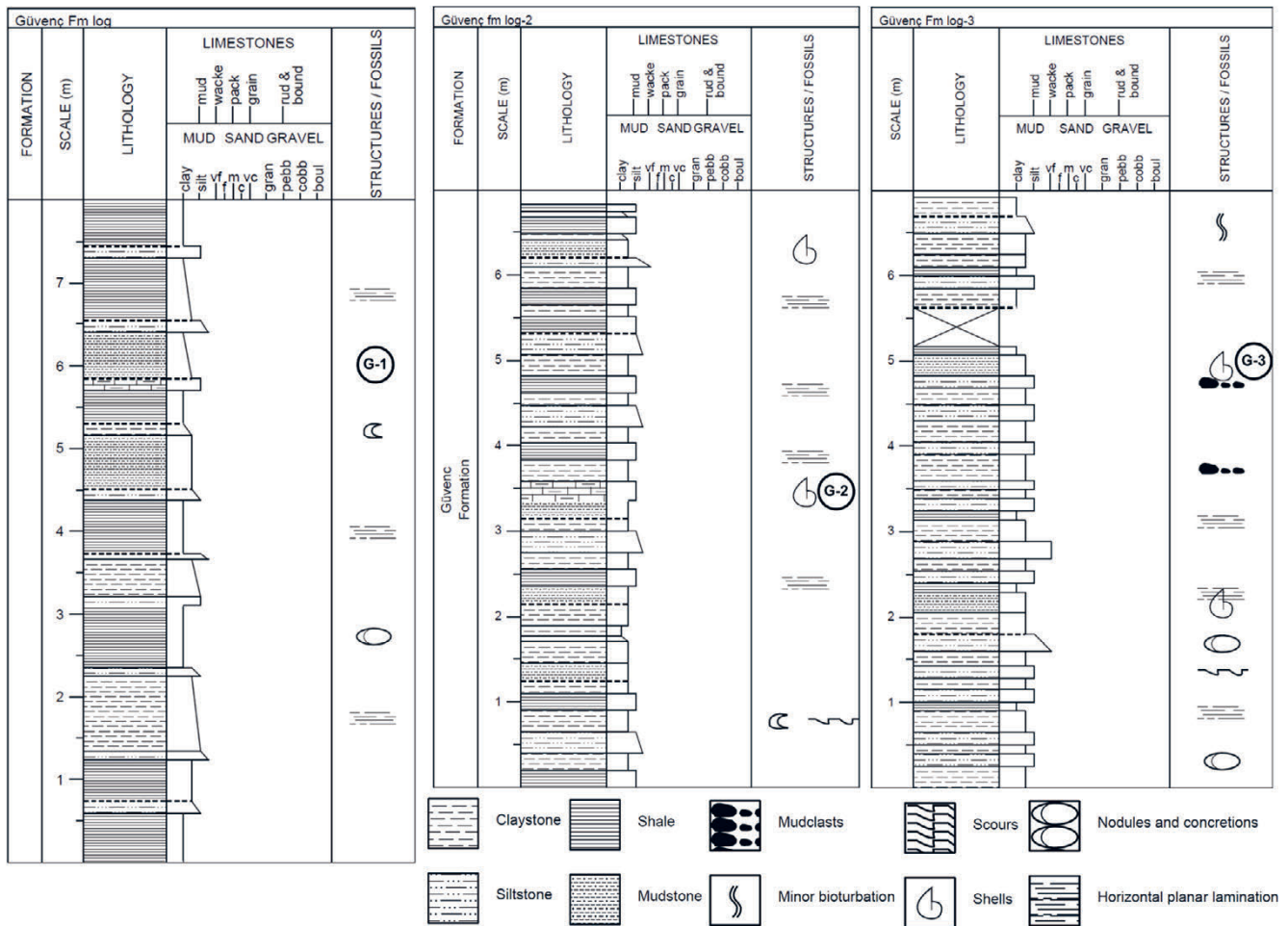


**Figure 10.** Sedimentological logs measured from the Güvenç Formation showing the levels of the sampling for Sr analysis (G-1,2,3) (see Figure 1 for locations).

Formation consisting mainly of marls and mudstones. The studied and sampled section is shown in Figure 12.

The  $^{87}\text{Sr}/^{86}\text{Sr}$  results were not obtained for one of the two samples (T-1) compiled from the Late Miocene carbonates. The  $^{87}\text{Sr}/^{86}\text{Sr}$  results of the other sample yielded an age of  $7.3 \pm 2.1$  ma (Tortonian–Messinian) (Fig. 7b).

### 5.5. The Kuzgun Formation

Sedimentary logging of the Kuzgun Formation (Figs. 5f, 13) and sampling for strontium analysis were carried out along the road linking the northern parts of the Karahan neighbourhood in the north-eastern part of Adana city centre and the Kuzgun-Abdullu villages in the north. One sample (Kz-1) (36 S 693185.00 d E/ 4106400.00 m N) was milled from a bivalve shell collected from the fine clastic sediments at the lowermost levels of the formation, (Memişli member) and another sample selected from the Kuzgun member (Kz-2) representing the upper levels. Sample Kz-3 was prepared from a gastropod shell obtained from the deltaic-shallow marine clastic rocks of the Memişli member (36 S 687733.00 d E/4109777.00 m N). Sample Kz-1 was milled from a large oyster shell collected from the underlying fine-grained shallow marine-fluvial clastics of the Kuzgun member (36 S 687241.00 d E/4110947.00 m N).

The strontium isotope ages of three samples collected from different levels of the Kuzgun Formation are given in

Figure 6. While the Kz-1 sample indicates a Tortonian–early Messinian age ( $7.4 \pm 2$  Ma), the results for the Kz-2 and Kz-3 samples are inconsistent, suggesting Pliocene–Pleistocene ages ( $1 \pm 0.5$  Ma and  $1.3 \pm 0.7$  Ma).

### 5.6. Handere Formation

Sedimentary logging and sampling studies of the Handere Formation were carried out along road cuts and galleries along the Kabasakal, Şambayadı, and Karahan quarters located in the north-eastern part of Adana city centre. Two samples were selected for strontium analysis. Sample H-1 was obtained from the middle part of the formation stratigraphically (36 S 697669.00 d E/ 4103394.00 m N) and sample H-2 was collected near the uppermost levels (36 S 695176.00 d E / 4102323.00 m N). Both samples were collected from the limestone, clayey-limestone interbeds in the unit, however, the Sr isotope results for these samples were not successfully obtained from the laboratory.

## 6. GEOLOGICAL IMPLICATIONS AND DISCUSSION

### 6.1. Kaplankaya-Karaisalı Formations and L. Miocene Carbonates

The  $^{87}\text{Sr}/^{86}\text{Sr}$  ages of the Kaplankaya Formation exhibiting lateral and vertical transitions into the Karaisalı Formation,



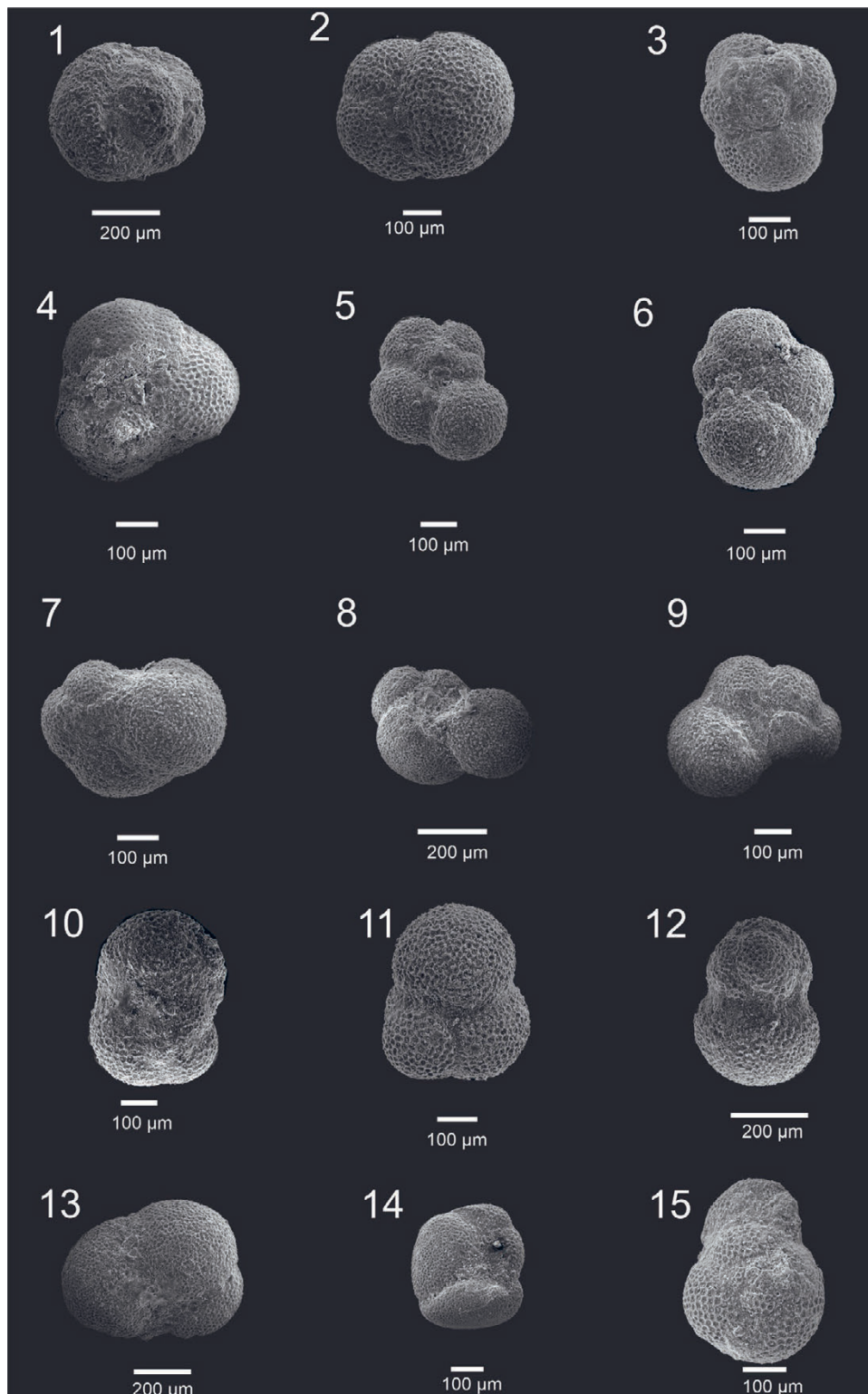


**Figure 11.** SEM images of the microfauna identified in the Güvenç Formation. 1 – *Globigerinoides bollii*; 2 – *Globigerinoides subquadratus*; 3 – *Globigerinoides* sp.; 4 – *Globigerinoides* sp.; 5 – *Globorotalia mayeri*; 6 – *Globorotalia mayeri*; 7 – *Globorotalia mayeri*; 8 – *Globigerinella obesa*; 9 – *Globigerinella obesa*; 10 – *Globigerinoides trilobus* (umbilical view); 11 – *Globigerinoides trilobus* (umbilical view); 12 – *Globigerinoides trilobus* (umbilical view); 13 – *Globigerinoides* cf. *Sacculifer*; 14 – *Globiquadrana dehiscens*; 15 – *Sphaeroidinellopsis* sp.

indicate Serravallian–Tortonian ages ( $9.5 \pm 2.4$  Ma to  $10 \pm 2.5$  Ma) (Fig. 7). Reported to contain abundant foraminifera such as *Borelis melo* FICHTEL & MOLL, *Borelis curdica* REICHEL, *Amphistegina* sp., and *Rotalia* sp., the Karaisalı Formation was palaeontologically assigned a Burdigalian–Langhian age (11–20 Ma) by SİREL & GÜNDÜZ (1981);

which makes our Sr isotope-derived ages slightly younger in comparison. ÜNLÜGENÇ & DEMİRKOL (1988) and ÖZALP (1993) assigned an early-middle Miocene age to the Kaplankaya Formation based on its fossil content compiled from the unit. The age data from the literature are, on average, several million years older than the  $^{87}\text{Sr}/^{86}\text{Sr}$  ages we obtained in this

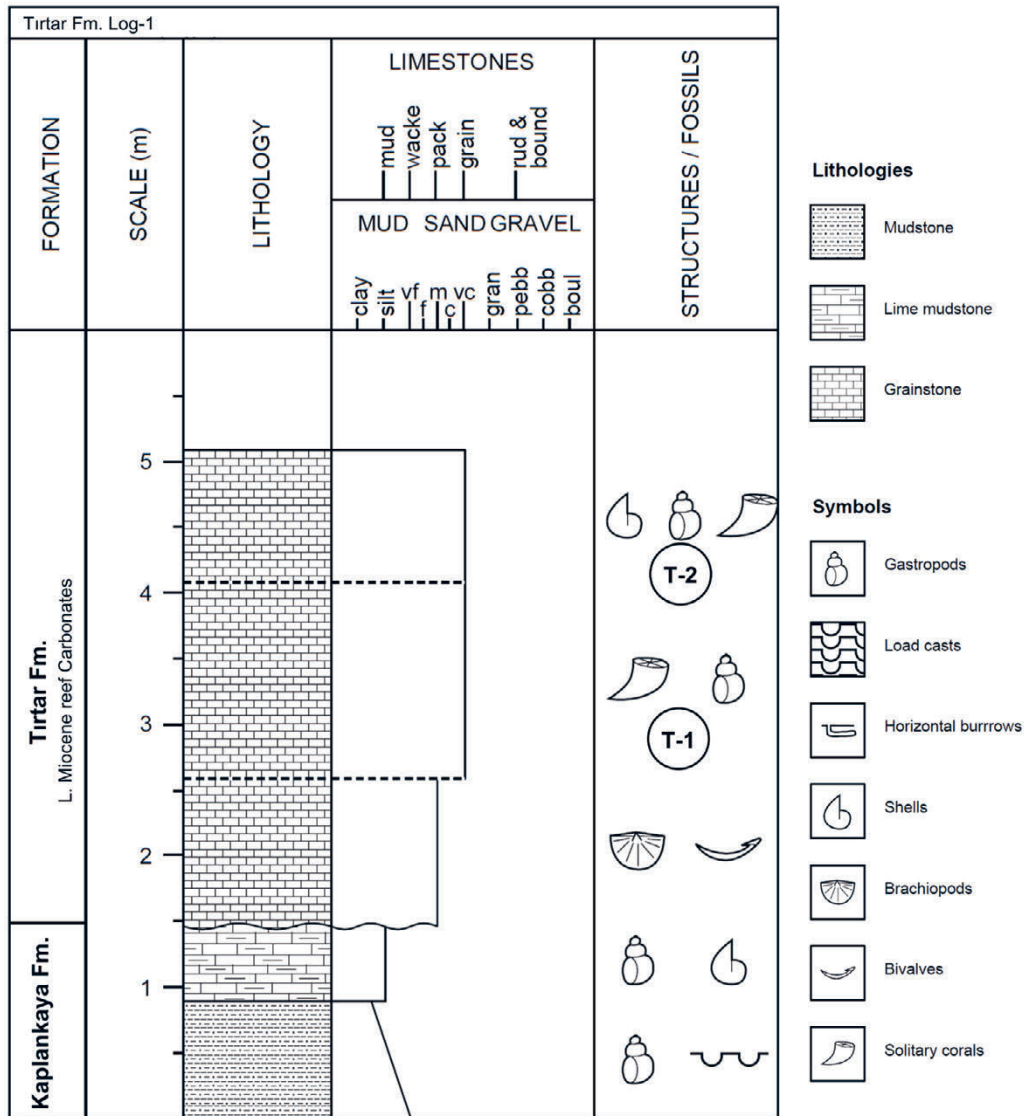


Figure 12. Sedimentological log of the Late Miocene reefal carbonates measured around the T-1 and T-2 sample site (see Figure 1 for location).

study. Since no significant diagenetic alteration was observed in the collected samples, two options can be considered to explain this low  $^{87}\text{Sr}/^{86}\text{Sr}$  ratio.

First, the age data obtained from these reef carbonates are consistent with the Tirtar Formation (middle-late Miocene reef carbonates), which is identified in the Mut Basin (ILGAR et al., 2013) located to the west of the Adana Basin. Therefore, these young reef sediments observed in the adjacent basin may have been deposited as thin layers over the slightly older Middle–Upper Miocene Karaisalı Formation in the western regions of the Adana Basin. The Sr isotope age data suggest that reef formation in the Adana Basin persisted not only in the Lower and Middle Miocene but also in the Upper Miocene. The carbonate rocks found south of the Karaisalı district which exhibit a patchy distribution in the Adana Basin, should be younger than the northern reef carbonates (Karaisalı Fm.), typically located at much higher elevations as steep cliffs. The shallow-marine and/or reefal carbonates of the Late Miocene were deposited directly on the Karaisalı and Kaplankaya formations by a short term transgression along the basin margin (Fig. 14).

A second option may be linked to continental run-off, although a minor influence from a secondary source to Kaplankaya/Karaisalı Formations deposited near the shoreline. Fluctuations in the  $^{87}\text{Sr}/^{86}\text{Sr}$  ratio in the catchment may be attributed to the influence of continental run-off derived low  $^{87}\text{Sr}/^{86}\text{Sr}$  weathered from the basement units including Palaeozoic–Mesozoic ophiolites and carbonate rocks.

Early marine diagenesis is also a critical stage in the diagenetic history of shallow-water carbonate sediments, significantly contributing to the transformation of metastable  $\text{CaCO}_3$  polymorphs, such as aragonite and high-Mg calcite, into the stable low-Mg calcite (HIGGINS et al., 2018). However, early marine diagenetic alteration is difficult to identify using either petrographic analysis or other conventional methods. AHM et al. (2018) developed a model that quantifies the resetting of  $\delta^{44/40}\text{Ca}$ ,  $\delta^{26}\text{Mg}$ ,  $\delta^{13}\text{C}$ , and  $\delta^{18}\text{O}$  in combination with elemental concentrations of Sr during neomorphism (aragonite-to-calcite), recrystallization (calcite-to-calcite), and dolomitization (calcite-to-dolomite). Various conventional techniques such as FTIR spectroscopy, XRD, and SEM are employed to differentiate between calcium carbonate polymorphs. Although SEM

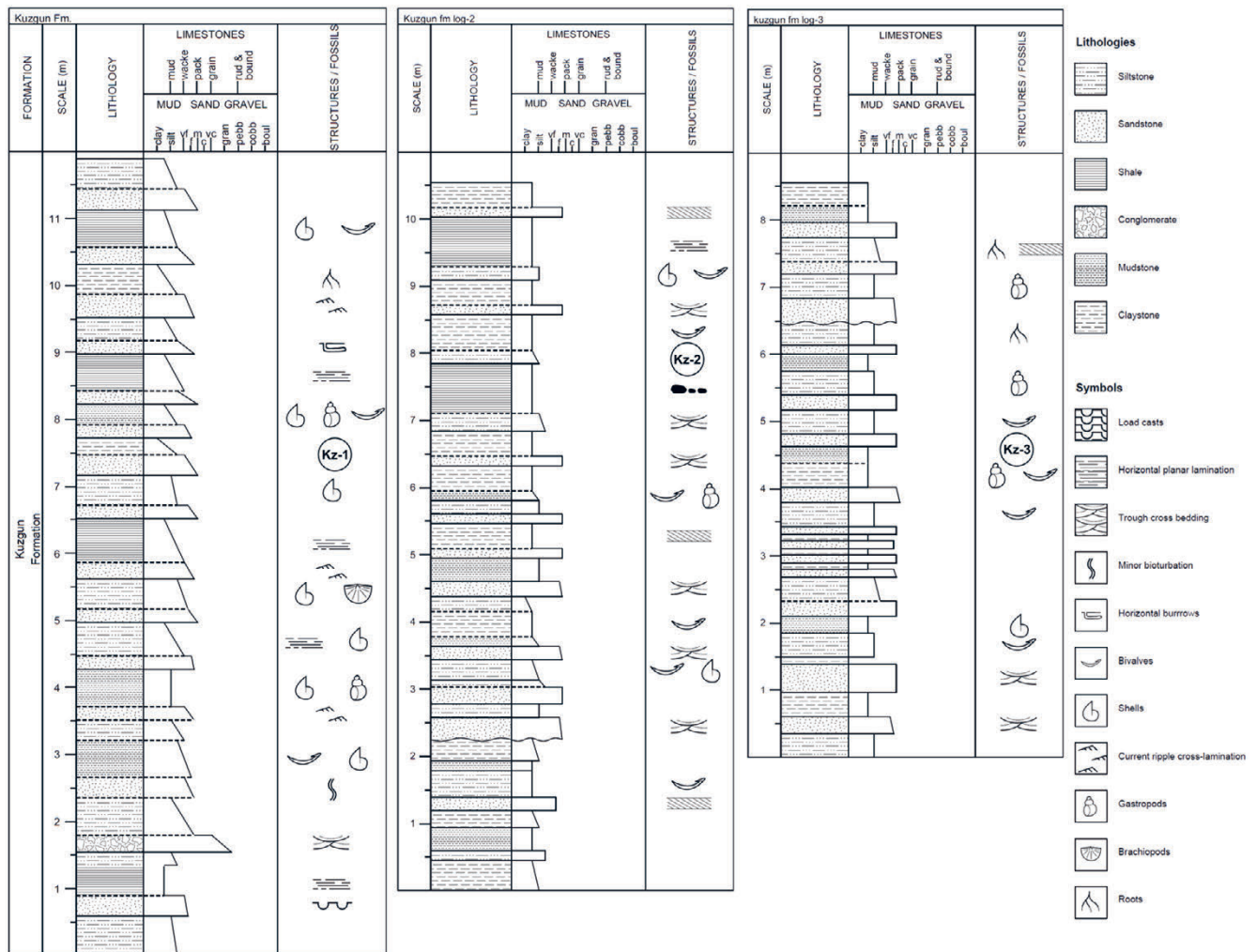


Figure 13. Sedimentological logs measured from the Kuzgun Formation showing the sample levels for Sr analysis (Kz-1,2,3) (see Figure 1 for locations).

analyses were conducted in this study, SEM does not provide definitive results in discerning calcium carbonate polymorph variations because the morphology of each calcium carbonate polymorph is not unique. However, the exact impact of this transformation on the geochemical composition of the rock remains to be fully elucidated.

## 6.2. The Cingöz and Güvenç Formations

The  $^{87}\text{Sr}/^{86}\text{Sr}$  analysis results of the Cingöz Formation (Table 2) yielded ages that range from  $23 \pm 1.3$  Ma (oldest) (Chatthian–Aquitanian) to  $12 \pm 2.1$  Ma (youngest) (Serravallian–Tortonian) (Fig. 10). According to the biostratigraphic literature, the Cingöz Formation has been assigned the following age ranges: Burdigalian to Serravallian (DEMİRTAŞLI & GENÇ, 1986), Langhian–Serravallian (GÖRÜR, 1979; YALÇIN & GÖRÜR, 1984) and Burdigalian–Langhian (YETİŞ & DEMİRKOL, 1986). A micro-palaeontological study carried out by NAZIK & GÜRBÜZ (1992) documented a comprehensive micro-fossil analysis of the entire turbiditic Cingöz Formation reporting that it was deposited during the late Burdigalian–Serravallian interval. A supportive fundamental biostratigraphic study was conducted in the locations where Sr sampling was carried out, as diagenetic alterations detected petrographically and geochemically in the samples could potentially cause

alterations of the original  $^{87}\text{Sr}/^{86}\text{Sr}$  compositions of the unit. The genera and species identified in the unit generally indicate the Burdigalian–?Serravallian interval (Fig. 9). It has been inferred that one of the three  $^{87}\text{Sr}/^{86}\text{Sr}$  age data is consistent with the literature ( $12 \pm 2.1$  Ma – Serravallian) and our biostratigraphic study; however, the other two Sr results (derived from lower parts of the unit) ( $22$ – $23$  Ma – Aquitanian) show a difference of approximately 3–4 M (older) from the proposed lower age limit for the unit. This situation may have occurred due to diagenetic alteration within the unit.

The  $^{87}\text{Sr}/^{86}\text{Sr}$  analyses of the Güvenç Formation indicate ages ranging from  $25 \pm 0.6$  Ma to  $16,9 \pm 0.9$  Ma corresponding to Chatthian–Langhian interval (Table 2, Fig. 7). However, biostratigraphic literature (NAZIK & TOKER, 1986; ÜNLÜGENÇ, 1993) provide Langhian–Serravallian (16–11 Ma) age for the unit. The palaeontological determinations made in this study also show that the age of the unit is Langhian–Serravallian. Thus, it was understood that there was a considerable difference in two out of three  $^{87}\text{Sr}/^{86}\text{Sr}$  ages (about 10 Ma) thought to be caused by diagenetic alteration (high Mg/Ca and Fe/Sr) in the Güvenç Formation similar to that observed in the Cingöz Formation, while one age data is roughly consistent with the biostratigraphical ages. The possibility that the Sr results, which are consistent with

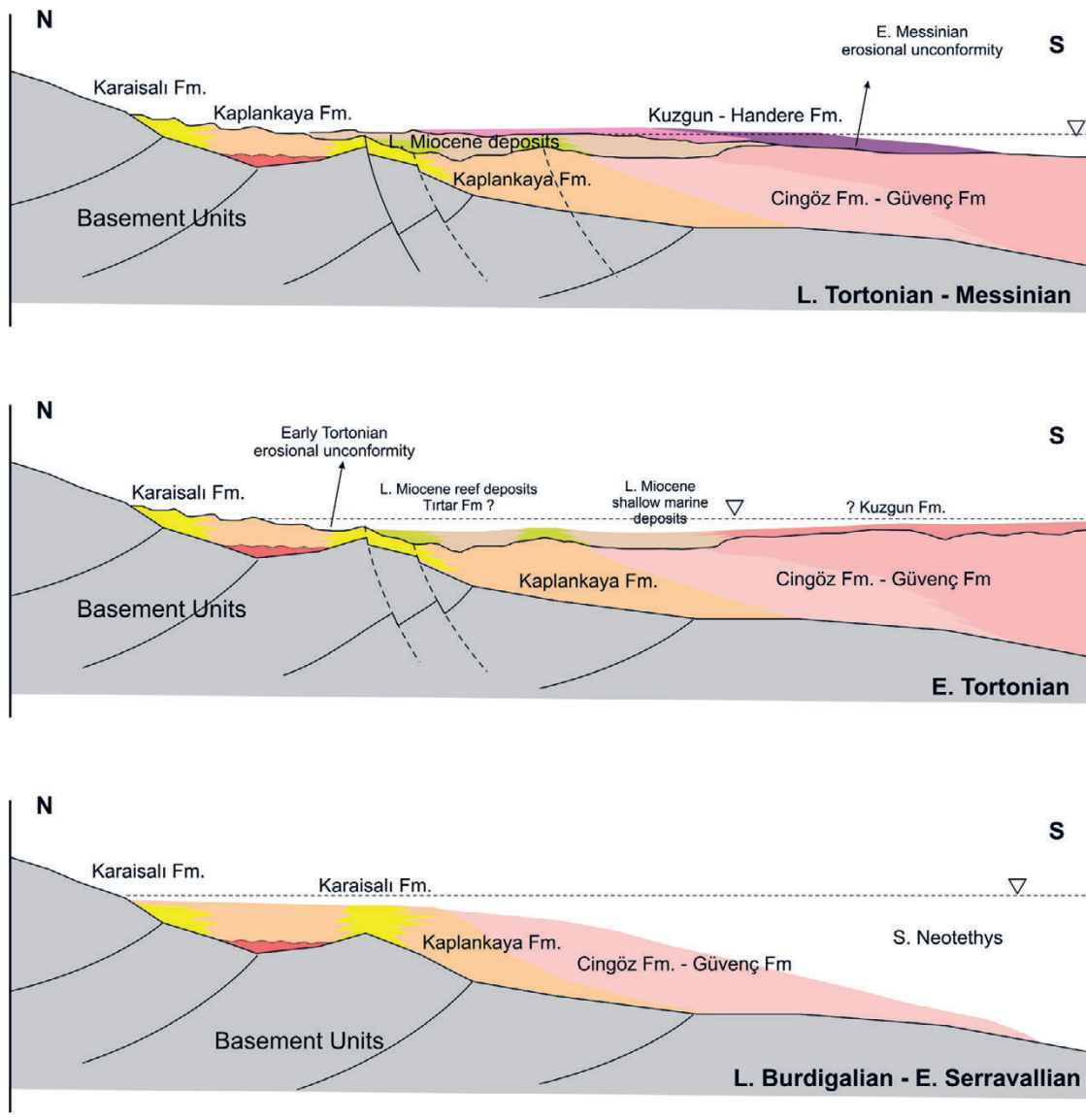


**Figure 14.** Schematic geological model summarising the inferred sedimentological development of the Adana Basin for Late Burdigalian to Messinian period.

biostratigraphic ages, also coincidentally provide coherent ages cannot be ignored. Correlations of prepared Sr isotope composition against Mn/Sr, Fe/Sr, Mg/Ca (Fig. 15) shows that there is no remarkable correlation between Sr isotope composition and Mn/Sr, while there is a moderately negative correlation between Mg/Ca and Fe/Sr. The decrease in Sr isotope ratios with the increase in Fe and Mn presented a significant negative linear correlation, which could explain the effect of contamination, especially for the Güvenç and Cingöz formations. Due to the sedimentary characteristics of the Güvenç and Cingöz formations that contain a high volume of detritus even at their carbonate dominated levels, and groundwater flow along their fractures, significant changes have occurred in their  $^{87}\text{Sr}/^{86}\text{Sr}$  composition. Since these units contain only sub-millimetre scale micro-fauna, they do not allow for a convenient Sr analysis using fossil shells.

Another important factor to consider in Sr isotope studies in the Eastern Mediterranean region is the highly complex

oceanographic evolution of the Mediterranean in the Miocene period. During this period, global and local controlling factors on seawater chemistry significantly influenced carbonate production related to the palaeoceanographic conditions of the Mediterranean and their changes over time. Aquitanian Sr and Nd isotope records of the Mediterranean indicate an open marine basin, influenced by the Indian Ocean and characterized by a predominant westward circulation, which is sensitive to global climate changes and carbon cycle disturbances. Starting from the late Burdigalian, the gradual shallowing and intermittent connection with the Indian Ocean altered the overall circulation in the basin, resulting in longer residence times of Mediterranean waters and reduced water exchanges not only with the Indian but also the Atlantic Oceans (KOCŞIS et al., 2008; CORNACCHIA et al., 2021). In this palaeoceanographic setting, regional factors such as volcanism had a greater effect on Mediterranean seawater chemistry compared to previous periods. Thus, the Sr isotope record of the Eastern Mediterranean could deviate towards lighter Sr isotope values.

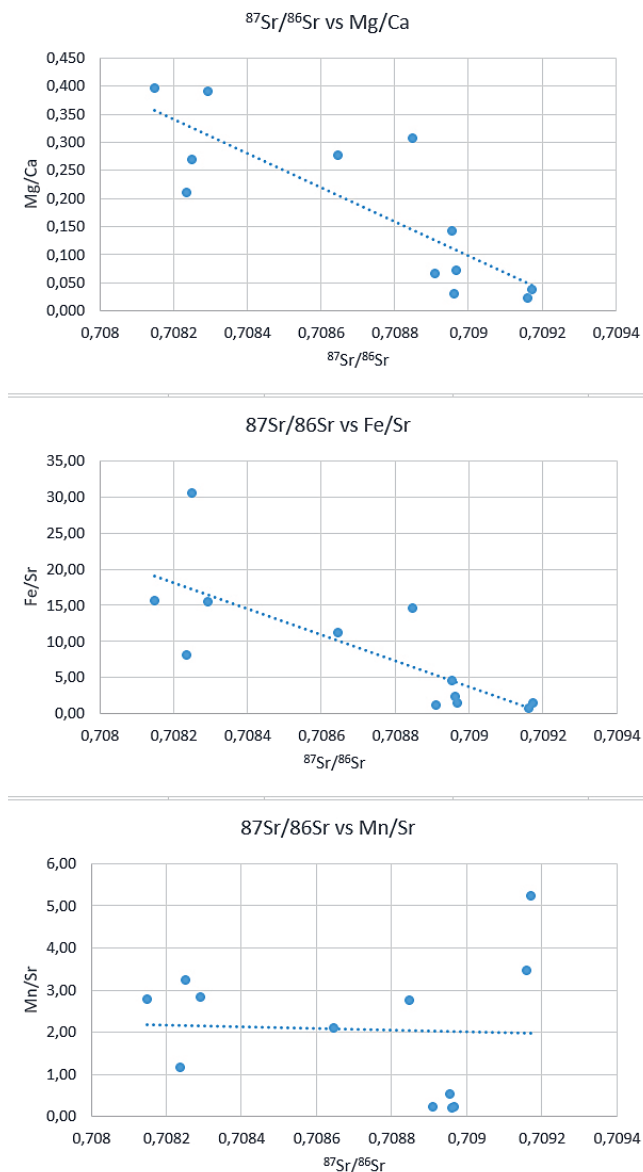


**Figure 15.** Diagrams (cartesian coordinates and trendlines) showing the correlation between Sr isotope composition versus Mn/Sr, Fe/Sr, Mg/Ca ratios for all the analysed samples.

### 6.3. The Kuzgun Formation

According to the  $^{87}\text{Sr}/^{86}\text{Sr}$  age data obtained from the basal levels of the Kuzgun Formation, the unit began to be deposited about  $7.4 \pm 2$  Ma. Inconsistencies were observed in the Sr ages of the Kuzgun Formation, analysed from the fossil shells. The Kz-1 sample points to the early Messinian, highly compatible with palaeontological literature (e.g., DARBAŞ & NAZİK, 2010; CIPOLLARI et al., 2013). A substantial biostratigraphical study of FARANDA et al. (2013) constrains the upper part of the Kuzgun Formation to the early Messinian. However, the results for the Kz-2 and Kz-3 samples are inconsistent and point to a Pleistocene age ( $\sim 1$  Ma). This could be due to several reasons. One probable cause is the change in strontium ratios due to the surface-alteration in the fossil shells (oyster/gastropod) where the sampling was made. However, geochemical analyses of the oyster and gastropod shell specimens (Kz-2 and Kz-3) collected from the unit yielded high Mn/Sr

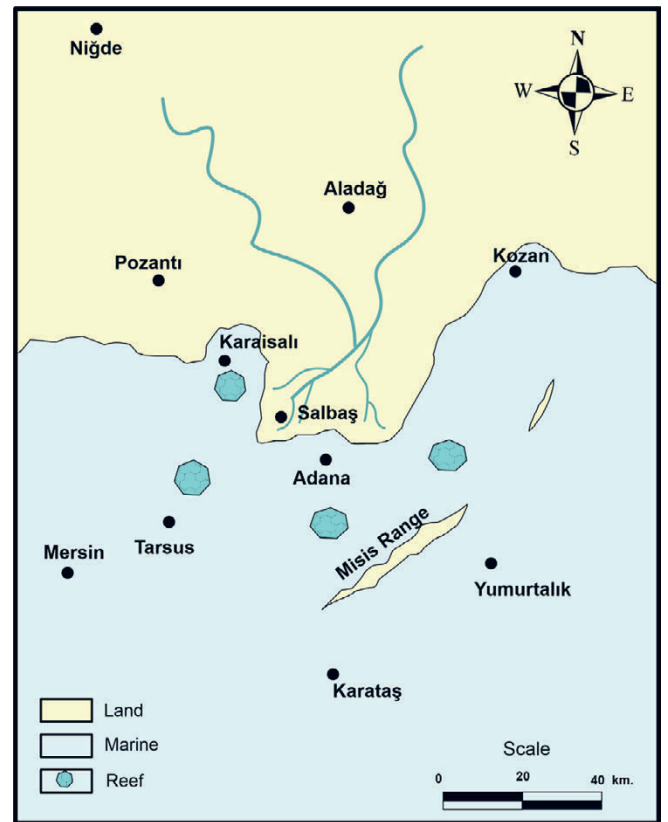


**Figure 16.** A simplified palinspastic map of the study region (Adana Basin) representing inferred environmental conditions during the Late Miocene.

ratios indicating that they were subjected to diagenetic alteration. On the other hand, if oyster shells are formed by calcite layers they can be suitable for Sr isotope dating but if they have porous shell layers and/or have irregular and chalky deposits this may cause deviations from the original Sr ratios (SCASSO et al., 2001). This high supergene manganese concentration, which is also reflected in the fossil shells, may be a clue to the distribution of manganese in the underlying parent rocks (FORCE & COX, 1991). Manganese may have been transported from depth to a surface of precipitation along local faults (STEAD & STOSE, 1943; COOPER, 1944). Mesozoic–Palaeozoic bedrocks of the Adana Basin including dolomitic rocks and quartzite (Demirkazık, Yerlikaya, Karahamzaşağı Formations) are the most likely candidates as sources of high Mn concentrations. Manganese enrichment in carbonates may also occur during the early diagenetic microbial reduction of manganese oxides (TORRES et al., 2014). The observed accumulation of manganese in these sediments is considered a significant indicator of early diagenetic microbial reduction, where anaerobic microbial communities utilize manganese oxides as electron acceptors in their metabolic processes. This reduction process, taking place in anaerobic environments, plays a pivotal role in influencing the cycling of manganese in marine sediments, consequently impacting the bioavailability of other essential nutrients. In such an anaerobic basin, iron precipitation can be associated with sulfate reduction and the metabolic activities of iron bacteria; during these processes, iron ( $\text{Fe}^{3+}$ ) is concurrently reduced and precipitates in an insoluble form, particularly through interactions among methanogenic and sulfate-reducing microorganisms.

$^{87}\text{Sr}/^{86}\text{Sr}$  ratios may deviate from the global reference curve due to restricted water exchange between a basin and the global ocean, which could be the case for the Upper Miocene succession of the Adana Basin. The deposition of the Handere and Kuzgun Formations was closely affected by the Lago-mare (Messinian) salinity crisis (from 5.96 to 5.33 Ma; KRIJGSMAN et al., 1996) in the Mediterranean during the late Miocene. The Lago-Mare scenario of terrestrial sedimentation in a dried-up Mediterranean basin has a unique base-level history and water chemistry of sub-basins (CIPOLLARI et al., 2013; MAILLARD et al., 2014; MICALLEF et al., 2019; CARUSO et al., 2020; KARTVEIT et al., 2019; MADOF et al., 2019; RAAD et al., 2021). A strontium influx into the lagoonal or lacustrine scenario was derived from drainage within each catchment. The  $^{87}\text{Sr}/^{86}\text{Sr}$  ratio of each water source is related to the lithologies weathered in the watersheds and the Sr ratio of the resulting basin reflects all these inputs (BATAILLE et al., 2012; DOEBBERT et al., 2014; BADDOUH et al., 2016). For the lagoonal scenario (ŞAFK et al., 2021), each individual basin receives an additional water source, which was supplied from the major peri-Mediterranean drainage systems (e.g., the Nile, Rhone, and Po; GRIFFIN, 2002) and, probably, the Atlantic as well (VASILIEV et al., 2017; GARCÍA-VEIGAS et al., 2018; GROTHE et al., 2020; ANDREETTO et al., 2021). By examining a significant number of  $^{87}\text{Sr}/^{86}\text{Sr}$  analyses conducted on oyster and foraminifera samples from the central and eastern Mediterranean basins, SCHILDGEN et al. (2014) suggest that a few million years before the Messinian Salinity Crisis,  $^{87}\text{Sr}/^{86}\text{Sr}$  in the basins fell below the global values, probably related to basin shallowing and tectonic uplift. During the Messinian Salinity Crisis, the composition of  $^{87}\text{Sr}/^{86}\text{Sr}$  from centrally located basins falls below global seawater values. This greater sensitivity to lowered sea level compared to higher continental flow may be related to the inverse relationship between Sr concentration and river discharge. CIPOLLARI et al. (2013) and FARANDA et al. (2013) have shown several evidence of the flooding and subsequent surface uplift in the Messinian–Zanclean period indicating that environmental conditions in the basin were quite unstable during this period.

Local volcanism in a region also generally tends to lower the Sr isotopic ratio due to injecting high amounts of light Sr. The volcanic/tuffitic level called the Salbaş tuffite member within the Kuzgun formation is exposed in the Adana Basin. The source of this volcanism was shown by NURLU et al. (2021) to be an area in the north, and it may have deviated the original Sr ratio in the units deposited during the Middle–Upper Miocene period. Although the authors determined ages ranging from 20 to 27 Ma, based on strontium age analysis for the carbonate-rich tuffite levels in the Kuzgun Formation, they suggested that they must have been deposited within an earlier marine basin originally, and then transported and re-deposited.

#### 6.4. The Handere Formation

$^{87}\text{Sr}/^{86}\text{Sr}$  data could not be obtained from the samples collected from the Handere Formation although they do not show any significant diagenetic alteration. Since this unit was generally deposited under terrestrial-transitional conditions, it can be thought that the terrestrial feed of the limited shallow marine

basin affected the natural strontium ratio. However, the 7 Ma age data obtained from the sample collected from the base levels of the overlying Kuzgun Formation, sheds light on the fact that the unit is younger than 7 Ma. Although the thin section analysis revealed no significant alteration traces, calcification known to be common throughout the unit has likely greatly affected the strontium content of the unit.

#### 7. CONCLUSION

This study presents the first integrated  $^{87}\text{Sr}/^{86}\text{Sr}$  chemo-geologic investigation for six different formations in the Adana Basin, where fifteen samples were systematically collected and analysed. According to the recorded  $^{87}\text{Sr}/^{86}\text{Sr}$  results, ages of  $9.5\pm 2.4$  Ma and  $10\pm 2.5$  Ma (Serravallian–Tortonian) were determined for the Kaplankaya/Karaisalı Formation, while ages of  $23\pm 1.3$  Ma (Chattian–Aquitania) to  $12\pm 2.1$  Ma (Serravallian) were found for the Cingöz Formation,  $25\pm 0.6$  Ma (Chattian) to  $16.9\pm 0.9$  Ma (Burdigalian–Tortonian) for the Güvenç Formation. The deviations in  $^{87}\text{Sr}/^{86}\text{Sr}$  results from the Cingöz and Güvenç formations, which are dominated by clastic deposits (marl), are attributed to diagenetic alteration diagnosed by geochemical analysis. Supportive biostratigraphical studies on these units showed that the ages of these units were Langhian–Serravallian and Burdigalian–Serravallian, respectively. The deviation in two out of three  $^{87}\text{Sr}/^{86}\text{Sr}$  age data obtained from the Kuzgun Formation may also be due to diagenetic alteration. It was determined that the thin reef carbonates, observed on an unconformity above the Kaplankaya Formation are Tortonian–Messinian ( $7.3\pm 2.1$  Ma) in age. This indicates that the marine conditions did not completely recede from the basin in the early Tortonian and marine influxes have taken place in short-term/multi-phases (episodic), resulting in the formation of younger reef sediments in the southern parts of the basin (Fig. 16). Although the recorded Sr isotopic data do not coincide well with the literature, this study provides an important basis for further detailed isotopic research in the region, highlighting the geological implications that were revealed.

#### ACKNOWLEDGEMENT

Author would like to thank the Department of Scientific Research Projects of Çukurova University (Adana, Turkey) for financial support for this study (Project No: FBA-2020-13028). For help on palaeontological study, I would like to thank Prof. Dr. Ümit ŞAFK and Hande SONSUN. Author would like to express sincere gratitude to the anonymous reviewers for their valuable feedback and constructive suggestions, which significantly contributed to the development of this paper.

#### REFERENCES

- AHM, A.-S.C., BJERRUM, C.J., BLÄTTLER, C.L., SWART, P.K. & HIGGINS, J.A. (2018): Quantifying early marine diagenesis in shallow-water carbonate sediments. – *Geochimica et Cosmochimica Acta*, 236, 140–159. <https://doi.org/10.1016/j.gca.2018.02.042>
- AKINCI, A.C. & ÜNLÜGENÇ, U.C. (2021): Neogene tectonic evolution of the Misis-Andırın-Engizek range: structural and sedimentary evidences from Bulgurkaya Sedimentary Mélange. – *Arabian Journal of Geosciences*, 14/7, 655. <https://doi.org/10.1007/s12517-021-06991-x>

- AKINCI, A.C., NURLU, N. & GÜNEY, A. (2023): Origin and geodynamic implications of basaltic rocks intercalated with Miocene turbidites around the Iskenderun Basin (Eastern Mediterranean/Turkey).– *Journal of African Earth Sciences*, 198, 104780. <https://doi.org/10.1016/j.jafrearsci.2022.104780>
- AL-AASM, I.S. & VEIZER, J. (1986): Diagenetic stabilization of aragonite and low-Mg calcite; I, Trace elements in rudists.– *Journal of Sedimentary Research*, 56, 138–152. <https://doi.org/10.1306/212F88A5-2B24-11D7-8648000102C1865D>
- ALBORA, A.M., SAYIN, N. & UÇAN, O.N. (2006): Evaluation of tectonic structure of Iskenderun Basin (Turkey) using steerable filters.– *Marine Geophysical Researches*, 27, 225–239. <https://doi.org/10.1007/s11001-006-9002-5>
- ANDREETTO, F., MATSUBARA, K., BEETS, C.J., FORTUIN, A.R., FLECKER, R. & KRIJGSMAN, W. (2021): High Mediterranean water-level during the Lago-Mare phase of the Messinian Salinity Crisis: insights from the Sr isotope records of Spanish marginal basins (SE Spain).– *Palaeogeography, Palaeoclimatology, Palaeoecology*, 562, 110139. <https://doi.org/10.1016/j.palaeo.2020.110139>
- ARGENTINO, C., REGHIZZI, M., CONTI, S., FIORONI, C., FONTANA, D. & SALOCCHI, A.C. (2017): Strontium isotope stratigraphy as a contribution for dating Miocene shelf carbonates (S. Marino Fm., northern Apennines).– *Rivista Italiana di Palaeontologia e Stratigrafia*, 123, 39–50.
- ASMEROM, Y., JACOBSEN, S.B., KNOLL, A.H., BUTTERFIELD, N.J. & SWETT, K. (1991): Strontium isotopic variations of Neoproterozoic Seawater: Implications for crustal evolution.– *Geochimica et Cosmochimica Acta*, 55, 2883–2894. [https://doi.org/10.1016/0016-7037\(91\)90453-C](https://doi.org/10.1016/0016-7037(91)90453-C)
- ATABEY, E., ATABEY, N., HAKYEMEZ, A., İSLAMOĞLU, Y., SÖZERI, Ş., ÖZÇELİK, N.N., SARAC, G., ÜNAY, E. & BABAYİĞİT, S. (2000): Lithostratigraphy and sedimentology of the Miocene Basin between Mut-Karaman [*Mut-Karaman arası Miyosen havzasının litostatigrafisi ve sedimentolojisi* – in Turkish].– *Bulletin of Mineral Research and Exploration*, 122, 53–72.
- BADDOUH, M.B., MEYERS, S.R., CARROLL, A.R., BEARD, B.L. & JOHNSON, C.M. (2016): Lacustrine  $^{87}\text{Sr}/^{86}\text{Sr}$  as a tracer to reconstruct Milankovitch forcing of the Eocene hydrologic cycle.– *Earth and Planetary Science Letters*, 448, 62–68.
- BARKA, A.A. & KADINSKY-CADE, K. (1988): Strike-slip fault geometry in Turkey and its influence on earthquake activity.– *Tectonics*, 7, 663–684. <https://doi.org/10.1029/TC007i003p00663>
- BATAILLE, C.P., LAFFOON, J. & BOWEN, G.J. (2012): Mapping multiple source effects on the strontium isotopic signatures of ecosystems from the circum-Caribbean region.– *Ecosphere*, 3, 1–24.
- BRAND, U. & VEIZER, J. (1980): Chemical diagenesis of a multicomponent carbonate system - I. Trace elements.– *Journal of Sedimentary Petrology*, 50, 1219–1236. <https://doi.org/10.1306/212f7bb7-2b24-11d7-8648000102c1865d>
- BRANDANO, M. & POLICICCHIO, G. (2012): Strontium stratigraphy of the Burdigalian transgression in the Western Mediterranean.– *Lethaia*, 45, 315–328. <http://doi.org/10.1111/j.1502-3931.2011.00285.x>
- BRASS, G.W. (1976): The variation of the marine  $^{87}\text{Sr}/^{86}\text{Sr}$  ratio during Phanerozoic time: interpretation using a flux model.– *Geochimica et Cosmochimica Acta*, 40, 721–730.
- BROEKER, W.S. & PENG, T.H. (1982): Tracers in the Sea.– *Eldigio Press Lamont Doherty Geological Observatory*, 690p.
- BURKE, W., DENISON, R., HETHERINGTON, E., KOEPNICK, R., NELSON, H. & OTTO, J. (1982): Variation of seawater  $^{87}\text{Sr}/^{86}\text{Sr}$  throughout Phanerozoic time.– *Geology*, 10, 516–519. [http://dx.doi.org/10.1130/0091-7613\(1982\)10%3C516:VOSSTP%3E2.0.CO;2](http://dx.doi.org/10.1130/0091-7613(1982)10%3C516:VOSSTP%3E2.0.CO;2)
- BURTON-FERGUSON, R., AKSU, A., CALON, T. & HALL, J. (2005): Seismic stratigraphy and structural evolution of the Adana Basin, eastern Mediterranean.– *Marine Geology*, 221, 189–222. <http://dx.doi.org/10.1016/j.margeo.2005.03.009>
- CAI, Y., YOU, C., WU, S., CAI, W. & GUO, L. (2020): Seasonal variations in strontium and carbon isotope systematics in the Lower Mississippi River: Implications for chemical weathering.– *Chemical Geology*, 553, 119810. <https://doi.org/10.1016/j.chemgeo.2020.119810>
- CARUSO, A., BLANC-VALLERON, M.M., DA PRATO, S., PIERRE, C. & ROUCHY, J.M. (2020): The late Messinian “Lago-Mare” event and the Zanclean reflooding in the Mediterranean Sea: New insights from the Cuevas del Almanzora section (Vera Basin, South-Eastern Spain).– *Earth-Science Reviews*, 200, 102993. <https://doi.org/10.1016/j.earscirev.2019.102993>
- CIPOLLARI, P., COSENTINO, D., RADEFF, G., SCHILDGEN, T.F., FARANDA, C., GROSSI, F., GLIOZZI, E., SMEDILE, A., GENNARI, R., DARBAŞ, G., DUDAS, F., GÜRBÜZ, K., NAZIK, A. & ECHTLER, H. (2013): Easternmost Mediterranean evidence of the Zanclean flooding event and subsequent surface uplift: Adana Basin, southern Turkey.– *Geological Society of London Special Publications*, 372, 615. <https://doi.org/10.1144/SP372.5>
- COOPER, B.N. (1944): Geology and mineral resources of the Burkes Garden quadrangle, Virginia.– *Virginia Geological Survey Bulletin*, 60, 299 p.
- CORNACCHIA, I., BRANDANO, M. & AGOSTINI, S. (2021): Miocene palaeoceanographic evolution of the Mediterranean area and carbonate production changes: A review.– *Earth-Science Reviews*, 221, 103785. <https://doi.org/10.1016/j.earscirev.2021.103785>
- DARBAŞ, G. & NAZIK, A. (2010): Micropalaeontology and palaeoecology of the Neogene sediments in the Adana Basin (South of Turkey).– *Journal of Asian Earth Sciences*, 39/3, 136–147. <https://doi.org/10.1016/j.jseaes.2010.03.002>
- DEMİRTAŞLI, E. & GENÇ, M. (1986): Final Report of the tectonic investigation between the Akkuyu site, Silifke-Mersin-Tarsus coastal area, Adana and Iskenderun basins, Ecemiş Fault Zone, Bolkar Mountains, Ereğli-Ulukışla basins and eastern part of the Mut Basin.– *General Directorate of Mineral Research and Exploration*, 59, 248 p.
- DERMAN, A.S. & GÜRBÜZ, K. (2007): Nature, provenance and relationships of early Miocene palaeovalley fills, northern Adana Basin, Turkey: their significance for sediment-bypassing on a carbonate shelf.– *Turkish Journal of Earth Sciences*, 16, 181–209.
- DERRY, L.A., KAUFMAN, A.J. & JACOBSEN, S.B. (1992): Sedimentary cycling and environmental change in the Late Proterozoic: Evidence from stable and radiogenic isotopes.– *Geochimica et Cosmochimica Acta*, 56, 1317–1329. [https://doi.org/10.1016/0016-7037\(92\)90064-P](https://doi.org/10.1016/0016-7037(92)90064-P)
- DEWEY, J.F. & ŞENGÖR, A.M.C. (1979): Aegean and surrounding regions: Complex multiplate and continuum tectonics in a convergent zone.– *GSA Bulletin*, 90, 84–92. [https://doi.org/10.1130/0016-7606\(1979\)90<84:AA-SRCM>2.0.CO;2](https://doi.org/10.1130/0016-7606(1979)90<84:AA-SRCM>2.0.CO;2)
- DEWEY, J.F., HEMPTON, M.R., KIDD, W.S.F., ŞAROĞLU, F. & ŞENGÖR, A.M.C. (1986): Shortening of continental lithosphere: The neotectonics of Eastern Anatolia – a young collision zone.– *Geological Society of London Special Publications*, 19, 404. <https://doi.org/10.1144/GSL.SP.1986.019.01.22>
- DOEBBERT, A.C., JOHNSON, C.M., CARROLL, A.R., BEARD, B.L., PIETRAS, J.T., CARSON, M.R., NORSTED, B. & THROCKMORTON, L.A. (2014): Controls on Sr isotopic evolution in lacustrine systems: Eocene green river formation, Wyoming.– *Chemical Geology*, 380. <https://doi.org/10.1016/j.chemgeo.2014.04.008>
- ELDERFIELD, H. (1986): Strontium isotope stratigraphy.– *Palaeogeography, Palaeoclimatology, Palaeoecology*, 57, 71–90. [https://doi.org/10.1016/0031-0182\(86\)90007-6](https://doi.org/10.1016/0031-0182(86)90007-6)
- FARANDA, C., GLIOZZI, E., CIPOLLARI, P., GROSSI, F. & DARBAŞ, G. (2013): Messinian palaeoenvironmental changes in the easternmost Mediterranean Basin: Adana Basin, southern Turkey.– *Turkish Journal of Earth Sciences*, 22, 839–863. <https://doi.org/10.3906/yer-1205-11>
- FLECKER, R. & ELLAM, R. (2006): Identifying Late Miocene episodes of connection and isolation in the Mediterranean–Parathyan realm using Sr isotopes.– *Sedimentary Geology*, 188, 189–203. <https://doi.org/10.1016/j.sedgeo.2006.03.005>
- FORCE, E.R. & COX, L.J. (1991): Manganese contents of some sedimentary rocks of Palaeozoic age in Virginia.– *United States Geological Survey*, 1916, 42. <https://doi.org/10.3133/b1916>

- GARCÍA-VEIGAS, J., CENDÓN, D.I., GIBERT, L., LOWENSTEIN, T.K. & ARTIAGA, D. (2018): Geochemical indicators in Western Mediterranean Messinian evaporites: implications for the salinity crisis.– *Marine Geology*, 403, 197–214. <http://dx.doi.org/10.1016/j.margeo.2018.06.005>
- GEALEY, W.K. (1988): Plate tectonic evolution of the Mediterranean-Middle East region.– *Tectonophysics*, 155, 285–306. [https://doi.org/10.1016/0040-1951\(88\)90270-3](https://doi.org/10.1016/0040-1951(88)90270-3)
- GLEASON, J.D., MOORE, T.C., REA, D.K., JOHNSON, T.M., OWEN, R.M., BLUM, J.D., HOVAN, S.A. & JONES, C.E. (2002): Ichthyolith strontium isotope stratigraphy of a Neogene red clay sequence: calibrating eolian dust accumulation rates in the central North Pacific.– *Earth and Planetary Science Letters*, 202, 625–636. [https://doi.org/10.1016/S0012-821X\(02\)00827-0](https://doi.org/10.1016/S0012-821X(02)00827-0)
- GOROKHOV, I., SEMIKHATOV, M.A. & BASKAKOV, A.V. (1995): Sr isotopic composition in Riphean, Vendian, and Lower Cambrian carbonates from Siberia.– *Stratigrafiya Geologicheskaya Korrelyatsiya*, 3, 3–33.
- GÖRÜR, N. (1979): Sedimentology of the Karaisalı Limestone [*Karaisalı kireçtaşının (Miyosen) sedimentolojisi* – in Turkish].– *Bulletin of the Geological Society of Turkey*, 22, 227–234.
- GRIFFIN, D.L. (2002): Aridity and humidity: two aspects of the late Miocene climate of North Africa and the Mediterranean.– *Palaeogeography, Palaeoclimatology, Palaeoecology*, 182, 65–91. [https://doi.org/10.1016/S0031-0182\(01\)00453-9](https://doi.org/10.1016/S0031-0182(01)00453-9)
- GROTHER, A., ANDREETTO, F., REICHHART, G.J., WOLTERS, M., VAN BAAK, C.G.C., VASILIEV, J., STOICA, M., SANGIORGI, F., MIDDELBURG, J.J., DAVIES, G.R. & KRIJGSMAN, W. (2020): Paratethys pacing of the Messinian Salinity Crisis: Low salinity waters contributing to gypsum precipitation?– *Earth and Planetary Science Letters*, 532, 116029. <https://doi.org/10.1016/j.epsl.2019.116029>
- GÜRBÜZ, K. (1985): Karaomerli-Akkuyu-Balcılı Bölgesi (N.Adana) Tersiyer istifinin sedimanter jeolojik incelenmesi.– *Çukurova Üniversitesi Fen Bilimleri Enstitüsü, M.Sc.Thesis* – in Turkish, 77 p.
- HEMPTON, M. (1985): Structure and deformation history of the Bitlis Suture near Lake Hazar, SE Turkey.– *Geological Society of America Bulletin*, 96. <https://doi.org/10.1130/0016-7606>
- HIGGINS, J.A., BLÄTTLER, C.L., LUNDSTROM, E.A., SANTIAGO-RAMOS, D.P., AKHTAR, A.A., CRÜGER AHM, A.S., BIALIK, O., HOLMDEN, C., BRADBURY, H., MURRAY, S.T. & SWART, P.K. (2018): Mineralogy, early marine diagenesis, and the chemistry of shallow-water carbonate sediments.– *Geochimica et Cosmochimica Acta*, 220, 512–534. <https://doi.org/10.1016/j.gca.2017.09.046>
- HODELL, D.A. (1994): Editorial: Progress and paradox in strontium isotope stratigraphy.– *Palaeoceanography*, 9, 395–398. <https://doi.org/10.1029/94PA00291>
- HODELL, D.A. & WOODRUFF, F. (1994): Miocene strontium isotope record of DSDP Hole 30-289 – Supplement to: HODELL, D.A. & WOODRUFF, F. (1994): Variations in the strontium isotopic ratio of seawater during the Miocene: Stratigraphic and geochemical implications.– *Palaeoceanography*, 9, 405–426. <https://doi.org/10.1029/94PA00292>
- HOWARTH, R. & MCARTHUR, J. (1997): Statistics for Strontium Isotope Stratigraphy: A robust lowess fit to the marine Sr-Isotope curve for 0 to 206 Ma, with look-up table for derivation of numeric age.– *The Journal of Geology*, 105, 441–456. <https://doi.org/10.1086/515938>
- ILGAR, A., NEMEC, W., HAKYEMEZ, A. & KARAKUŞ, E. (2013): Messinian forced regressions in the Adana Basin: a near-coincidence of tectonic and eustatic forcing.– *Turkish Journal of Earth Sciences*, 22/5, 864–889. <https://doi.org/10.3906/yer-1208-3>
- JONES, C.E. & JENKYN, H.C. (2001): Seawater strontium isotopes, oceanic anoxic events, and seafloor hydrothermal activity in the Jurassic and Cretaceous.– *American Journal of Science* 301, 112–149. <http://dx.doi.org/10.2475/ajs.301.2.112>
- KAHLE, H.G., COCARD, M., PETER, Y., GEIGER, A., REILINGER, R., BARKA, A. & VEIS, G. (2000): GPS-derived strain rate field within the boundary zones of the Eurasian, African, and Arabian Plates.– *Journal of Geophysical Research: Solid Earth*, 105, 23353–23370. <https://doi.org/10.1029/2000JB900238>
- KARTVEIT, K.H., ULSUND, H.B. & JOHANSEN, S.E. (2019): Evidence of sea level drawdown at the end of the Messinian salinity crisis and seismic investigation of the Nahr Menashe unit in the northern Levant Basin, offshore Lebanon.– *Basin Research*, 31, 827–840. <https://doi.org/10.1111/bre.12347>
- KAUFMAN, A.J., JACOBSEN, S.B. & KNOLL, A.H. (1993): The Vendian record of Sr and C isotopic variations in seawater: Implications for tectonics and palaeoclimate.– *Earth and Planetary Science Letters*, 120/3–4, 409–430. [https://doi.org/10.1016/0012-821X\(93\)90254-7](https://doi.org/10.1016/0012-821X(93)90254-7)
- KELLING, G., GÖKÇEN, S.L., FLOYD, P.A. & GÖKÇEN, N. (1987): Neogene tectonics and plate convergence in the eastern Mediterranean: New data from southern Turkey.– *Geology*, 15, 425–429. [https://doi.org/10.1130/0091-7613\(1987\)15<425:NTAPCI>2.0.CO;2](https://doi.org/10.1130/0091-7613(1987)15<425:NTAPCI>2.0.CO;2)
- KOCSIS, L., VENNEMANN, T.W., FONTIGNIE, D., BAUMGARTNER, C., MONTANARI, A. & JELEN, B. (2008): Oceanographic and climatic evolution of the Miocene Mediterranean deduced from Nd, Sr, C, and O isotope compositions of marine fossils and sediments.– *Palaeoceanography*, 23, PA4211. <https://doi.org/10.1029/2007PA001540>
- KOEPNICK, R.B., BURKE, W.H., DENISON, R.E., HETHERINGTON, E.A., NELSON, H.F., OTTO, J.B. & WAITE, L.E. (1985): (Appendix 1) Biostratigraphy and Sr isotopic composition of sediments from DSDP Hole 17-167 (dataset). <https://doi.org/10.1594/PANGAEA.706575>
- KOEPNICK, R.B., DENISON, R. & DAHL, D. (1988): The Cenozoic seawater  $^{87}\text{Sr}/^{86}\text{Sr}$  curve: data review and implications for correlation of marine strata.– *Palaeoceanography*, 3, 743–756. <http://dx.doi.org/10.1029/PA003i006p00743>
- KÖKSAL, S. (2019): The Upper Cretaceous intrusive rocks with extensive crustal contribution in Hacimahmutuşağı Area (Aksaray/Turkey).– *Geologica Carpathica*, 70, 261–276. <http://dx.doi.org/10.2478/geoca-2019-0015>
- KRIJGSMAN, W., GARCÉS, M., LANGEREIS, C., DAAMS, R., DAM, J., MEULEN, A.V.D., AGUSTÍ, J. & CABRERA, L. (1996): A new chronology for the middle to late Miocene continental record in Spain.– *Earth and Planetary Science Letters*, 142, 367–380. [http://dx.doi.org/10.1016/0012-821X\(96\)00109-4](http://dx.doi.org/10.1016/0012-821X(96)00109-4)
- KUZNETSOV, A.B., GOROKHOV, I., SEMIKHATOV, M.A., MELNIKOV, N.N. & KOZLOV, V.I. (1997): Strontium isotopic composition from the Inzer Formation limestones, the Upper Riphean type section in southern Urals.– *Transactions of the Russian Academy of Sciences, Earth Science Sections*, 353, 319–324.
- KUZNETSOV, A.B., SEMIKHATOV, M.A., GOROKHOV, I.M., MELNIKOV, N.N., KONSTANTINOVE, G.V. & KUTYAVIN, E.P. (2003): Sr isotope composition in carbonates of the Karatau Group, Southern Urals, and standard curve of  $^{87}\text{Sr}/^{86}\text{Sr}$  variations in the Late Riphean Ocean.– *Stratigr. Geological Correlation*, 11, 415–449.
- KUZNETSOV, A.B., SEMIKHATOV, M.A. & GOROKHOV, I.M. (2012): The Sr isotope composition of the world ocean, marginal and inland seas: Implications for the Sr isotope stratigraphy.– *Stratigraphy and Geological Correlation*, 20, 501–515. <https://doi.org/10.1134/S0869593812060044>
- MADOF, A.S., BERTONI, C. & LOFI, J. (2019): Discovery of vast fluvial deposits provides evidence for drawdown during the late Miocene Messinian salinity crisis.– *Geology*, 47, 171–174. <https://doi.org/10.1130/g45873.1>
- MAHMOUD, Y., MASSON, F., MEGHRAOUI, M., ÇAKIR, Z., ALCHALBI, A., YAVAŞOĞLU, H., YÖNLÜ, O., DAOUD, M., ERGINTAV, S. & İNAN, S. (2013): Kinematic study at the junction of the East Anatolian fault and the Dead Sea fault from GPS measurements.– *Journal of Geodynamics*, 67, 30–39. <https://doi.org/10.1016/j.jog.2012.05.006>
- MAILLARD, A., DRIUSSI, O., LOFI, J., BRIAIS, A., CHANIER, F., HUEBSCHER, C. & GAULLIER, V. (2014): Record of the Messinian salinity crisis in the SW Mallorca area (Balearic Promontory, Spain).– *Marine Geology*, 357, 304–320. <http://dx.doi.org/10.1016/j.margeo.2014.10.001>
- MCARTHUR, J.M. (1994): Recent trends in strontium isotope stratigraphy.– *Terra Nova*, 6, 331–358. <https://doi.org/10.1111/j.1365-3121.1994.tb00507.x>



- MCARTHUR, J.M., HOWARTH, R.J. & BAILEY, T.R. (2001): Strontium Isotope Stratigraphy: LOWESS Version 3: Best fit to the marine Sr-isotope curve for 0–509 Ma and accompanying look-up table for deriving numerical age.— *The Journal of Geology*, 109, 155–170. <https://doi.org/10.1086/319243>
- MCARTHUR, J.M., HOWARTH, R.J. & SHIELDS, G.A. (2012): Strontium Isotope Stratigraphy.— In: GREDSTEIN F.M., OGG, J.G., SCHMOTZ, M.D. & OGG, G.M. (eds.): *A Geologic Time Scale*, Elsevier, Amsterdam, 127–144. <http://dx.doi.org/10.1016/b978-0-444-59425-9.00007-x>
- MICALLEF, A., CAMERLENGHI, A., GEORGIPOULOU, A., GARCIA-CASTELLANOS, D., GUTSCHER, M.A., IACONO, C., HUVENNE, V.A.I., MOUNTJOY, J.J., PAULL, C.K., BAS, T., SPATOLA, D., FACCHIN, L. & ACCETTELLA, D. (2019): Geomorphic evolution of the Malta Escarpment and implications for the Messinian evaporative drawdown in the eastern Mediterranean Sea.— *Geomorphology*, 327, 264–283. <https://doi.org/10.1016/j.geomorph.2018.11.012>
- MILLER, K.G., FEIGENSON, M.D., WRIGHT, J.D. & CLEMENT, B.M. (1991): Miocene isotope reference section, Deep Sea Drilling Project Site 608: An evaluation of isotope and biostratigraphic resolution.— *Palaeoceanography*, 6, 33–52. <https://doi.org/10.1029/90PA01941>
- NAZIK, A., & GÜRBÜZ, K. (1992): Planktonic foraminiferal biostratigraphy of Lower-Middle Miocene aged submarine fans in Karaisalı-Çatalan-Eğner region (NW Adana).— *Turkish Geology Bulletin*, 35, 67–80.
- NAZIK, A. & TOKER, V. (1986): Foraminiferal biostratigraphy of the Middle Miocene succession in the Karaisalı region.— *Mineral Research Exploration Journal*, 103, 139–150.
- NURLU, N., TÜRKMEN, S., AKINCI, A.C. & ŞAFK, Ü. (2021): Strontium isotope geochronology and geochemical provenance of a volcanoclastic sequence (Salbaş member) in the Adana Basin (southern Turkey).— *Arabian Journal of Geosciences*, 14, 1634. <https://doi.org/10.1007/s12517-021-07624-z>
- OSLICK, J.S., MILLER, K.G., FEIGENSON, M.D. & WRIGHT, J.D. (1994): (Table 1) Age model of ODP hole 120-747A (dataset). <https://doi.org/10.1594/PANGAEA.52657>
- ÖZALP, S. (1993): Stratigraphy of the Gülek-Çamalan (Tarsus) area.— *Yerbilimleri-Geosound*, 22, 73–84.
- ÖZÇELİK, N. & YETİŞ, C. (1994): Adana Basin Tertiary sequence Planktic foraminiferal biostratigraphy of the Güvenç Formation.— *Yerbilimleri*, 25, 21–30.
- PERİNÇEK, D. & ÇEMEN, İ. (1990): The structural relationship between the East Anatolian and Dead Sea fault-zones in SE Turkey.— *Tectonophysics*, 172, 331–340. [https://doi.org/10.1016/0040-1951\(90\)90039-B](https://doi.org/10.1016/0040-1951(90)90039-B)
- RAAD, F., LOFI J., MAILLARD, A., TZEVAHIRTZIAN, A. & CARUSO, A. (2021): The Messinian Salinity Crisis deposits in the Balearic Promontory: An undeformed analog of the MSC Sicilian Basins?— *Marine and Petroleum Geology*, 124, 104777. <https://doi.org/10.1016/j.marpetgeo.2020.104777>
- REILINGER, R., MCCLUSKY, S., PARADISSIS, D., ERGINTAV, S. & VERNANT, P. (2010): Geodetic constraints on the tectonic evolution of the Aegean region and strain accumulation along the Hellenic subduction zone.— *Tectonophysics*, 488, 22–30. <https://doi.org/10.1016/j.tecto.2009.05.027>
- ROBERTSON, A.H.F. (1998): Mesozoic–Tertiary tectonic evolution of the easternmost Mediterranean area: integration of marine and land evidence.— In: ROBERTSON, A.H.F., EMEIS, K.C., RICHTER, C. & CAMERLENGHI, A. (eds): *Proceedings of the Ocean Drilling Program: Scientific Results*, 160, 723–782.
- ROBERTSON, A.H.F. & DIXON, J.E. (1984): Introduction: aspects of the geological evolution of the Eastern Mediterranean.— *Geological Society London Special Publications*, 17. <https://doi.org/10.1144/GSL.SP.1984.017.01.02>
- SCASSO, R.A., MCARTHUR, J., DEL RIO, C., MARTINEZ, S. & THIRLWALL, M. (2001): <sup>87</sup>Sr/<sup>86</sup>Sr Late Miocene age of fossil molluscs in the ‘Entrerriense’ of the Valdés Peninsula (Chubut, Argentina).— *Journal of South American Earth Sciences*, 14, 319–329.
- SCHILDGEN, T.F., COSENTINO, D., FRIJIA, G., CASTORINA, F., DUDAS, F.Ö., IADANZA, A., SAMPALMIERI, G., CIPOLLARI, P., CARUSO, A., BOWRING, S.A. & STRECKER, M.R. (2014): Sea level and climate forcing of the Sr isotope composition of late Miocene Mediterranean marine basins.— *Geochemistry Geophysics Geosystems*, 15, 2964–2983. <https://doi.org/10.1002/2014GC005332>
- SCHMIDT, G.C. (1961): Stratigraphic nomenclature for the Adana region petroleum district VII.— *Petroleum Administration Bull. Ankara* 6, 47–63.
- SCHNEIDER, S., FÜRSTICH, F.T. & WERNER, W. (2009): Sr-isotope stratigraphy of the Upper Jurassic of central Portugal (Lusitanian Basin) based on oyster shells.— *International Journal of Earth Sciences*, 98, 1949–1970. <http://dx.doi.org/10.1007/s00531-008-0359-3>
- SEMIKHATOV, M.A., GOROKHOV, I., KUZNETSOV, A.B., MEL’NILIV, N.N., PODKOVOYROV, V. & KISLOVA, I.V. (1998): Sr isotopic composition in early late Riphean sea water: Limestones of the Lakhanda group, the Uhur-Maya region, Siberia.— *Doklady Akademii Nauk*, 360, 236–240.
- SINACI, M. (2010): Nanoplankton biostratigraphy and environmental characteristics of Miocene-Pleistocene succession with drilling data in Adana basin.— Ankara University, PhD Thesis, 250 p.
- SIREL, E. & GÜNDÜZ, H. (1981): Description of new Borelis species from the Hatay (S. of Turkey) and Elazığ region (E. of Turkey).— *Mineral Research Exploration Institute Turkey*, 92, 70–74.
- STEAD, F.W. & STOSE, G.W. (1943): Manganese and quartzite deposits in the Lick Mountain district, Wythe County, Virginia.— *Virginia Geological Survey Bulletin*, 59, 16 p.
- ŞAFK, Ü. & ÜNLÜGENÇ, U.C. (1992): Ostracoda fauna and biostratigraphy of Oligocene–Lower Miocene succession cropping out around Kozoluk, Solaklı and Kevizli (N of Adana) [*Kozoluk, Solaklı ve Kevizli (Adana k’i) civarında yüzeyleyen Oligosen-orta Miyosen yaşlı istiflerin ostrakod faunası ve biostratigrafisi* – in Turkish].— *Yerbilimleri (Geosound)*, 21, 117–139.
- ŞAFK, Ü., AKINCI, A.C. & SONUN, H. (2021): Ostracod fauna and palaeoenvironmental characteristics of the tuffite and Memişli succession in the Fadıl and Salbaş region (Adana/Turkey).— *Journal of Engineering Sciences of Adıyaman University*, 8, 179–195.
- ŞENGÖR, A.M.C. (1979): Mid-Mesozoic closure of Permo–Triassic Tethys and its implications.— *Nature*, 279, 590–593. <http://dx.doi.org/10.1038/279590a0>
- ŞENGÖR, A.M.C. & YILMAZ, Y. (1981): Tethyan evolution of Turkey: A plate tectonic approach.— *Tectonophysics*, 75, 181–190. [http://dx.doi.org/10.1016/0040-1951\(81\)90275-4](http://dx.doi.org/10.1016/0040-1951(81)90275-4)
- TARAF, F., EREN, M. & GÜRBÜZ, K. (2013): Facies and microfacies features of the Karaisalı Formation (Adana Basin-Türkiye).— *Geology Bulletin of Turkey*, 56, 173–188.
- TORRES, N., OCH, L., HAUSER, P., FURRER, G., BRANDL, H., VOLOGINA, E., STURM, M., BÜRGMANN, H. & MÜLLER, B. (2014): Early diagenetic processes generate iron and manganese oxide layers in the sediments of Lake Baikal, Siberia.— *Journal of Environmental Monitoring*, 16, 879–889. <http://dx.doi.org/10.1039/c3em00676j>
- ULLMANN, C.V., CAMPBELL, H.J., FREI, R., HESSELBO, POGGE VON STRANDMANN, S.P. & KORTE, C. (2013): Partial diagenetic overprint of Late Jurassic belemnites from New Zealand: Implications for the preservation potential of  $\delta^{7}\text{Li}$  values in calcite fossils.— *Geochimica et Cosmochimica Acta*, 120, 80–96. <https://doi.org/10.1016/j.gca.2013.06.029>
- ÜNLÜGENÇ, U.C. (1986): The Geology of the Kızıldağ Plateau (Adana) Area [*Kızıldağ Yayla (Adana) Dolayının Jeolojisi Ç.Ü.* – in Turkish].— *Fen Bilimleri Enstitüsü, MSc. Thesis, Adana*, 77 p.
- ÜNLÜGENÇ, U.C. (1993): Controls on Cenozoic Sedimentation, Adana Basin southern Turkey.— *Ph.D. Thesis, University of Keele*, 228 p.
- ÜNLÜGENÇ, U.C. & AKINCI, A.C. (2020): Sedimentary characteristics of early Miocene platform deposits in the Neogene Adana Basin, southern Turkey.— *Turkish Journal of Earth Sciences*, 29, 629–648. <http://dx.doi.org/10.3906/yer-1910-20>

- ÜNLÜGENÇ, U.C. & DEMIRKOL, C. (1988): Stratigraphy of the Surroundings of Kızıldağ Yayla (Adana) [*Kızıldağ Yayla (Adana) dolayımın stratigrafisi* – in Turkish].– *Jeoloji Mühendisliği*, 32, 17–25.
- ÜNLÜGENÇ, U.C. & ŞAFAK, Ü. (1992): Environmental interpretation of the early Miocene Deposits (Kaplankaya Formation) in the Adana Basin, S. Türkiye.– *Yerbilimleri*, 20, 363.
- ÜNLÜGENÇ, U.C., AKINCI, A.C. & KARAKILÇIK, H. (2019): Sedimentary evidences for the depositional and environmental changes regarding to regression during Mid to Late Miocene in the Neogene Adana Basin (Southern Turkey).– *Journal of Engineering and Architecture*, 34, 1–8. <http://dx.doi.org/10.21605/cukurovaummfd.702008>
- VASILIEV, I., MEZGER, E.M., LUGLI, S., REICHART, G.J., MANZI, V. & ROVERI, M. (2017): How dry was the Mediterranean during the Messinian salinity crisis?– *Palaeogeography, Palaeoclimatology, Palaeoecology*, 471, 120–133. <https://doi.org/10.1016/j.palaeo.2017.01.032>
- VEIZER, J. (1983): Trace elements and isotopes in sedimentary carbonates.– *Reviews in Mineralogy and Geochemistry*, 11, 265–299.
- VESCOGNI, A., BOSELLINI, F.R., CIPRIANI, A., GÜRLER, G., ILGAR, A. & PAGANELLI, E. (2014): The Dağpazarı carbonate platform (Mut Basin, Southern Turkey): Facies and environmental reconstruction of a coral reef system during the Middle Miocene Climatic Optimum.– *Palaeogeography, Palaeoclimatology, Palaeoecology*, 410, 213–232. <http://dx.doi.org/10.1016/j.palaeo.2014.05.040>
- WIERZBOWSKI, H. (2013): Strontium isotope composition of sedimentary rocks and its application to chemostratigraphy and palaeoenvironmental reconstructions.– *Annales UMCS, Sectio AAA: Physica*, 68. <http://doi.org/10.2478/v10246-012-0017-2>
- YALÇIN, M.N. & GÖRÜR, N. (1984): Sedimentological evolution of the Adana basin.– In: TEKELİ, O. & GÖNCÜOĞLU, M.C. (eds.): *Geology of the Taurus Belt: Proceedings of International Symposium*, Ankara, Turkey, 26–29, 125–142.
- YANG, S., JIANG, S., LING, H., XIA, X., SUN, M. & WANG, D. (2007): Sr–Nd isotopic compositions of the Changjiang sediments: Implications for tracing sediment sources.– *Science in China Series D-Earth Sciences*, 50, 1556–1565. <https://doi.org/10.1007/s11430-007-0052-6>
- YETİŞ, C. (1988): Reorganisation of the Tertiary stratigraphy in the Adana Basin, Southern Turkey.– *Newsletter Stratigraphy*, 20, 43–58.
- YETİŞ, C. & DEMIRKOL, C. (1986): Detailed Study of the Western Part of the Adana Basin [*Adana Baseni Batı kesiminin detay etüdü* – in Turkish].– MTA Report, 8037, 187 p. (unpublished).
- YETİŞ, C., DEMIRKOL, C. & KEREY, E. (1986): Facies and environmental characteristics of the Kuzgun formation (Upper Miocene) of the Adana Basin.– *Bulletin of the Geological Society of Turkey*, 29, 81–96.
- YILMAZ, Y. (1993): New Evidence and Model on the Evolution of the Southeast Anatolian Orogen.– *Geological Society of America Bulletin*, 105, 251–271. [https://doi.org/10.1130/0016-7606\(1993\)105<0251:NEA-MOT>2.3.CO;2](https://doi.org/10.1130/0016-7606(1993)105<0251:NEA-MOT>2.3.CO;2)